International
Progress Report

IPR-03-50

Äspö Hard Rock Laboratory

TRUE-1 Continuation project

Fault rock zones characterisation

Preliminary structural-geological description of target structures based on borehole data and tunnel mapping

Lars Mærsk Hansen
Jan Hermanson
Isabelle Staub
Golder Associates AB

Eva-Lena Tullborg
Terralogica AB

November 2003

Svensk Kärnbränslehantering AB
Swedish Nuclear Fuel
and Waste Management Co
Box 5864
SE-102 40 Stockholm Sweden
Tel 08-459 84 00
+46 8 459 84 00
Fax 08-661 57 19
+46 8 661 57 19

Äspö Hard Rock
Laboratory

Report no.
IPR-03-50
No.
F83K
Author
Lars Mærsk Hansen
Jan Hermanson
Isabelle Staub
Eva-Lena Tullborg
Date
November 2003
Checked by
Anders Winberg
Date
2007-10-08
Approved
Christer Svemar
Date
2007-10-22

Äspö Hard Rock Laboratory

TRUE-1 Continuation project

Fault rock zones characterisation

Preliminary structural-geological description of target structures based on borehole data and tunnel mapping

Lars Mærsk Hansen
Jan Hermanson
Isabelle Staub
Golder Associates AB

Eva-Lena Tullborg
Terralogica AB

November 2003

Keywords: Epoxy, Fault rock zones, Mapping, Overcoring, Pore space

Abstract

16 exploratory 76 mm cored boreholes, evenly distributed at four fault rock zones localities along the Äspö ramp, were completed and characterized. Information from the drilling together with information from tunnel mapping of associated tunnel sections were used to assess the usefulness of the various localities and boreholes for injection of epoxy resin in targeted fault rock zones structures with subsequent overcoring and analyses. Geological materials were used for preliminary assessment of the mineralogy and geochemistry of selected fault rock zones.

The evaluation of the information from the boreholes/drill cores from the four structures at 1/600 m, 2/163 m, 2/430 m and 2/545 m supports the suitability of three structures (the ones at 1/600 m, 2/163 m and 2/430 m) for epoxy resin injections. The ‘zone 2545’, in contrast, shows a more complex geometry and it is not recommended to include this structure in subsequent resin injection experiments.

Sammanfattning

16 kärnborrhål (76 mm), jämt fördelade på 4 utvalda lokaler med sprickzoner (fault rock zones) längs Äspötunneln, borrades och karakteriserades. Informationen från borrhålen och från kartering av aktuella tunnelavsnitt användes för att bedöma lämplighet av berörda zoner och borrhål för injicering av epoxy med efterföljande överborrning och analys. Geologiskt material användes för en första bedömning av valda zoners mineralogi och geokemi.

Utvärderingen av informationen från borrhålen borrade på de fyra zonerna vid 1/600 m, 2/163 m, 2/430 m och 2/545 m stöder valet av zonerna vid 1/600 m, 2/163 m och 2/430 m för epoxy-injicering. Zonen vid 2/545 m uppvisar en mer komplex geometri och rekommenderas att inte ingå i fortsatta injiceringsexperiment med epoxy.

Contents

1 Background and Objective 9

2 Scope of Work 11

3 Model A. Tunnel Chainage 2/545 m 13

4 Model B. Tunnel Chainage 2/430 m 17

5 Model C. Tunnel Chainage 2/163 m 21

6 Model D. Tunnel Chainage 1/600 m 25

7 Mineralogy and geochemistry 29

8 Conclusions 30

9 References 33

Appendix 1: Photographs of tunnel sections and cores from each candidate site 35

Appendix 2: Detailed tabulations of findings in each of the drilled boreholes 43

A2a : Geometrical borehole data 45

A2b : Rock types 46

A2c : Fracture mapping 47

A2d : RQD 52

A2e : Details on fault zones 53

A2f : Water inflow 54

Appendix 3: Structural geological map of drill cores KA1596, KA2169, KA2423 and KA2549. 55

Appendix 4: Detailed geological map of the tunnel wall of each candidate zone 59

Appendix 5: ICP analysis of samples from KA1596A01, KA2169A02 and KA2423A03 65

Appendix 6: XRD analysis on samples from KA1596A01, KA2169A02 and KA2423A03 67

1 Background and Objective

The project aims to characterize the porosity of faults and fractures with respect to pore volume and geometry in order to identify which parts of a fracture or a fault that can carry water. The principal means of investigation is epoxy resin injection followed by overcoring. Supporting information is provided by various additional characterization tools and analysis techniques. Experience from Äspö HRL, Forsmark Nuclear Power Plant, Sikfors Hydroelectric Power Station, and many other sites show that water is not transported uniformly but along specific more or less irregular “channels” on a fracture plane or inside a fault.

Four target fault and fracture zones have been selected in the access tunnel to the Äspö Hard Rock Laboratory at Chainages 1/600, 2/163, 2/430 and 2/545. The four target structures and zones have been modeled at the four locations in the tunnel. A brief description of the target structures and the 3D RVS site models of the structures are presented and illustrated in /Stigsson et al., 2003/. The interpretation of structures has been made on tunnel observations and fracture mapping according to /Mazurek et al., 1997/.

In order to clarify the suitability of these structures for the purpose of the experiment core drillings were carried out at these 4 target locations. The boreholes are subhorizontal and their locations along the tunnel and their lengths were defined in order to drill through the four fault and fracture zones. Subsequently to drilling the holes were logged using the BIPS borehole imaging system in order to determine the orientation of fractures, thin veins and other structures. The observations of structures in the cores were used to confirm and update the model and description of the targeted structures.

Updated models of the fault and fracture zones helped to localize the depth of occurrence of structures in which epoxy resin should be injected, and to determine suitable depths to place the mechanical packer.

The epoxy-impregnated target faults or fracture zones will be overcored using a 300 mm drill bit, producing 277 mm overcores. Analysis of the overcores and the infillings is expected to give an understanding of the porosity texture.

Further description of the experiment is given in the Project Plan ”Characterisation of fault rock zones using epoxy resin injection” /Birgersson et al, 2002/.

2 Scope of Work

- Core drillings were carried out through four fault and fracture zones, in the access tunnel to the Äspö Hard Rock Laboratory at Chainages 1/600, 2/163, 2/430 and 2/545. Four short holes (from 2.93 to 5.94 metres) were drilled at each site representing in all 72.06 meters of drilled cores. 76-mm coring using triple tube was implemented, the innermost barrel being separated in two half-barrels in order to obtain good samples of fault gouge, breccia, and/or crushed materials.
- Photographs of zone exposures and drill cores were taken: whole box, half box, and zone details, as required. Selected photographs are shown in Appendix 1 (complete set of photographs have been delivered separately on a CD).
- Cores were logged tentatively with respect to rock type, fractures and their angles relative to the core axis, and RQD. The results are reported in tables in Appendix 2.
- Zone intersections in cores were mapped in detail, usually at scale 1:2. The results are shown in Appendix 3.
- At each site the zones were mapped in detail with respect to master faults, fault material, lithology where relevant, and adjacent fractures such as splay cracks, as described by /Mazurek et al., 1997/. The results are presented in Appendix 4.
- Each borehole was also BIPS logged, providing orientation of structures such as mylonites, faults and fractures.
- Each borehole was surveyed in order to obtain the accurate location, bearing and plunge of the hole.
- Pre-existing mapping of the tunnel walls and roof was judged to have an accuracy in position within 1 to 2 metres which is not sufficient for this project. Therefore the evidences of geological structures in the tunnel have been surveyed with a high accuracy better than 2 cm using a total station in order to obtain an accurate input to the RVS modelling.
- The four site models previously constructed in RVS were updated on the basis of new more accurate tunnel survey and borehole observations. The north arrow in the figures refers to the north of the Äspö96 coordinate system which has a bearing of 348° from magnetic north. Strike and dip of structures are given in relation to magnetic north.

Below follows a description of each of the identified candidate sites for resin injection. In addition to the site descriptions there are four Appendices detailing the following;

Appendix 1: Photographs of tunnel sections and cores from each candidate site.

Appendix 2: Detailed table of findings in each of the drilled boreholes.

Appendix 3: Structural geological map of drill cores KA1596, KA2169, KA2423 and KA2549.

Appendix 4: Detailed geological map of the tunnel wall of each candidate zone.

Appendix 5: ICP analysis of samples from KA1596A01, KA2169A02 and KA2423A03.

Appendix 6: XRD analysis on samples from KA1596A01, KA2169A02 and KA2423A03.

3 Model A. Tunnel Chainage 2/545 m

The identified structure at this site occurs in the ceiling of the tunnel at chainage 2/545 m. The structure as interpreted before drilling, referred to as ‘zone 2545’, strikes NW 307° and dips NE 65° /Stigsson et al., 2003/. See Appendix 4 for a detailed geological map of the tunnel wall.

The new survey of the tunnel in conjunction to the drilling campaign highlighted the inaccuracy of the measurements of zone locations on the tunnel wall. Therefore the zone was remodeled prior to drilling based on new survey data. The remodeled structure strikes 303.2° and dips 89.6°, see (Figure 3-1).

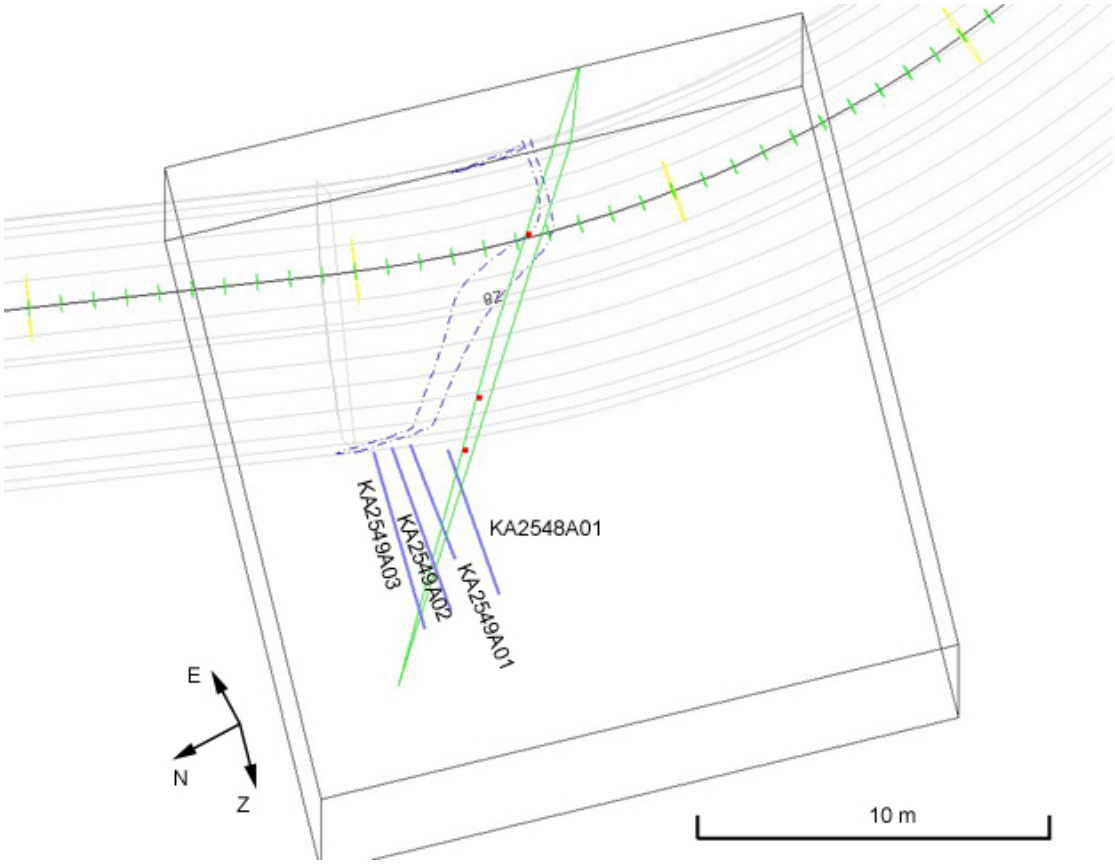

Figure 3-1. *The model of ‘zone 2545’ as interpreted before drilling but using data from the new tunnel survey. The red points illustrate the tunnel intercepts of the zone used for the modelling.*

NW-striking features are often encountered in the Äspö tunnels and they are often water conductors. Some of them are characterised by crushed rock and breccia. Hence the activities at this site aim to characterize the NW striking fracture identified at the site.

Four boreholes, KA2548A01, KA2548A02, KA2548A03 and KA2549A01 were drilled from the tunnel at the location of the interpreted target structure (Figure 3-1).

The rock identified in the boreholes is mainly granodiorite to diorite (Äspö diorite), with subordinate red, fine-grained granite and occasional cataclasite, pegmatite and aplite, see Appendix 3. RQD varies between 81 and 98.

In the tunnel the structure appears to terminate against a steeply dipping fracture striking NNE, which is crossing the tunnel ceiling at 2/550 m, see Figure 3-2. This was confirmed during drilling of KA2549A01 where a shear plane, featuring narrow breccias, striking 235° and dipping 65-70° was identified at a depth of ca 2.1 meters (Figure 3-3). Beyond that shear zone other NW striking fractures are identified by BIPS logging, but none of them at a depth corresponding to the target fracture exposed in the tunnel. Thus, these fractures are not suitable for the experiment as epoxy resin will be administered in different fractures.

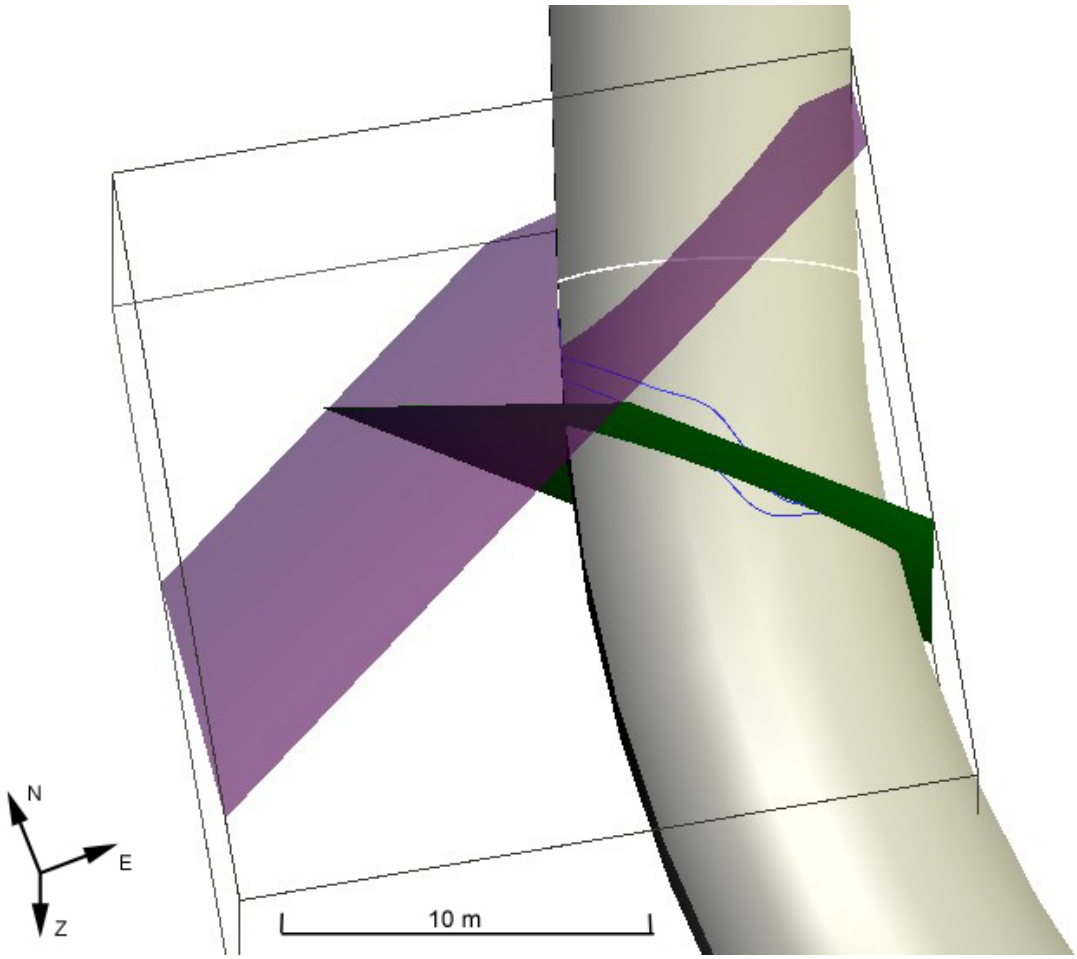

Figure 3-2. *Overview of the RVS model A. The target zone 'zone 2545' (green) terminates towards a narrow shear plane (transparent purple).*

The indication of a zone in KA2548A01 shows the characteristics of the NW structure and is associated to 'zone 2545' (Figure 3-3). Nevertheless, this fracture is located very close to the tunnel and is thus not suitable for the experiment.

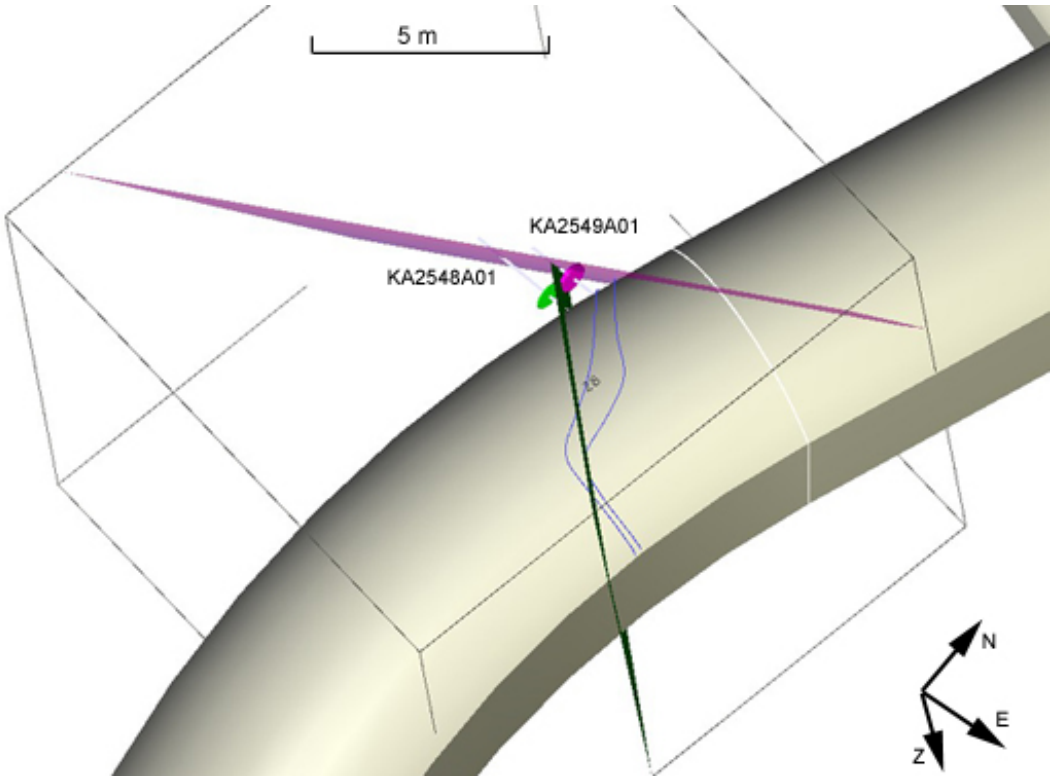

Figure 3-3. *RVS model A with borehole and fault geometry. View along 'zone 2545' intersection axis (crest of the tunnel, chainage 2/545 m). The purple disc shows an indication of the NNE shear zone, the green disc is an indication of a NW-striking feature.*

In boreholes KA2548A01, KA2549A01, and KA2548A03, no water flow at all was observed during and after drilling. In borehole KA2548A02 water could be observed after the last round, 3.88-5.21 m, and a flow of 950 ml/min was measured after completion of the drilling.

The 'zone 2545' is regarded as being a typical representative of the NW striking fracture swarms, with short fractures, offset by N-S or NE-SW structures.

As illustrated in Figure 3-3 indications of the shear zone are not found in KA2548A01 which might indicate that the zone changes direction to the north beyond KA2549A01 or that the zone has a limited extent.

Neither breccia nor fault gouge occur in the selected structure. As 'zone 2545'does not contain any loose material, and as the original target fracture does not extend beyond a crossing structure, as shown in Figure 3-2 and Figure 3-3, its character is regarded as not being within the scope of the present project, and is thus not recommended for resin injection experiments. The injection boreholes may be suitable for study of the "porosity" of a fracture zone or of very coarse (10-20 cm blocks) "crushed zone" rather than of what is usually regarded as fault material, such as fault crush, fault breccia or fault gouge.

4 Model B. Tunnel Chainage 2/430 m

The zone identified at this site intersects the tunnel crest line at chainage 2/430 m. The structure interpreted from existing tunnel data strikes NNW 341° and dips ENE 87° /Stigsson et al., 2003/. Its width varies from zero to 25 cm, and the material can be characterized as a cataclasite or mylonite, with unidentified hard minerals, see Appendix 4 for a detailed geological map of the tunnel wall.

More accurate measurements of the zone indications in the tunnel prior to drilling showed a slight discrepancy with the data used in the preceding modeling. The remodeled ‘zone 2430’ has an orientation of 338.4° / 85°.

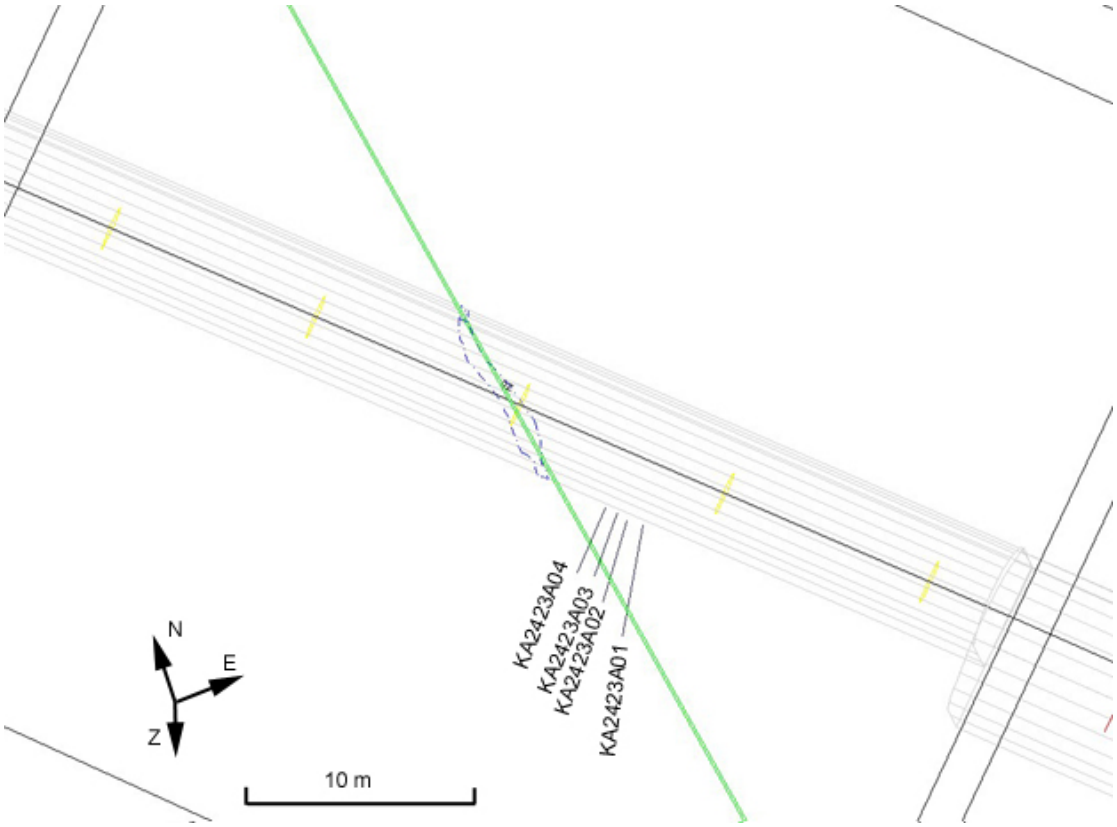

Figure 4-1. *Illustration of the zone occurrence in the tunnel and the points used for modelling the ‘zone 2430’ before drilling, and localisation of the boreholes.*

Four holes, KA2423A01, KA2423A02, KA2423A03 and KA2423A04 were drilled from the tunnel in the proximity of the target structure (Figure 4-1). The rock identified in the holes is mainly Småland Granite, and granodiorite (Äspö Diorite), see Appendix 3. RQD varies between 85 and 96 in the four exploration boreholes.

All four holes intercept fault breccia and crushed material in zones about 1-3 cm wide. The zone occurs in borehole KA2423A01 at 4.25 m, in borehole KA2423A02 at 2.75 m, in borehole KA2423A03 at ca 3.3 m, and in borehole KA2423A04 at ca 1.9 m (Figure 4-2).

In the cores the zone is located in protocataclasite and includes thin mylonites. It is characterized by repeated 1-2 cm wide sub-zones of fault breccia and subordinate fault crush. The material is flaky with green, hard, unidentified minerals. There are also a number of sub-horizontal fractures interpreted as splay cracks.

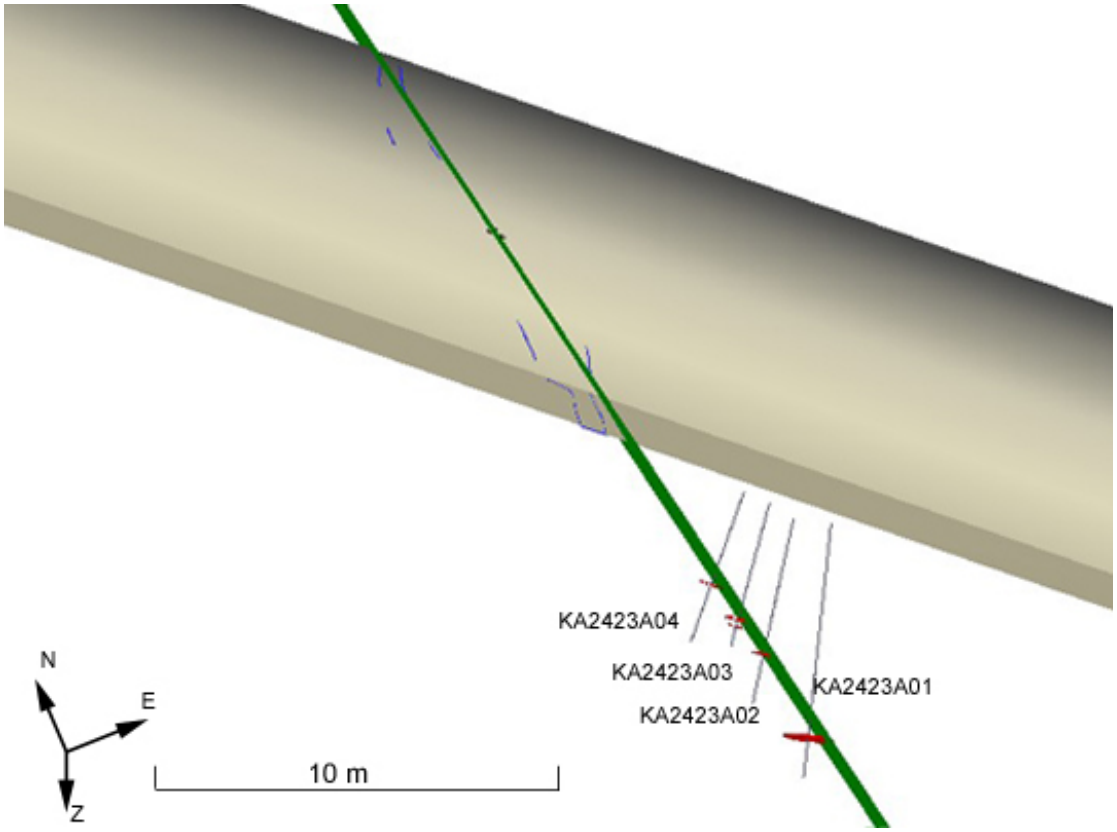

Figure 4-2. *RVS model B with visualisation of the zone occurrence in the boreholes and the fault geometry. The zone intersects the tunnel crest at chainage 2/430 m.*

The sub-zones are narrow, usually located in rock of good quality and do hence only marginally influence on the general quality of the rock mass, such as the RQD-value. They may however constitute a discontinuity, which can influence adversely on the local stability of an engineered structure, if such structure forms a footwall.

The zone appears to be a normal fault, considering the bend of the splay cracks, but there are no marker structures to show the magnitude of displacement.

The depth of occurrence in the boreholes and the orientation of the structures in the boreholes (as determined from BIPS logging) fit very well with the expected depths projected from the modeled structure, see Figure 4-2. The ‘zone 2430’ has therefore not been remodeled after drilling.

No water flow was observed in any borehole during drilling. Low water flows were measured after completion of drilling in boreholes KA2423A01 and KA2423A03, 23 and 13 ml/min, respectively.

All four boreholes feature fault breccia with a thickness of 1-3 cm and are regarded as being suitable for resin injection experiments for this type of fault rock material. Water flow is observed in 2 of the 4 holes which might imply that the zone carry some water. The fact that two boreholes are totally dry does not necessarily mean that the zone is non-conductive, but can be due to the vicinity of the drained zone close to the tunnel. In any case, 'zone 2430' gives an opportunity to study the variations in porosity and hydraulic conductivity within a few meters in the same structure.

This zone constitutes a reactivated epidote-rich mylonite hosted in red-stained and hydrothermally altered granite/granodiorite. The zone varies in width from 4 cm (KA2423A04) to 10 cm (KA2423A01). The structure is characterised at all four borehole intercepts by open pore spaces and fault crush. Sieved samples of the crushed material in the zone in KA2423A03 show the following grain size distribution (total sample 51.5 g): > 2 mm, 39 g; 1-2 mm, 4 g; 0.5-1 mm, 3 g; 0.25 mm-0.5 mm, 2 g; 0.25-0.125 mm, 2 g; and <0.125 mm,1.5 g. The amount of clay minerals in this structure is quite low compared to other zones ('zone 2163' and 'zone 1596'). An explanation might be that the cementation of the grains has been slightly more intense in this zone. An argument for this hypothesis is the observation of particles that look like clay-cemented grains in the 1-2- mm fraction. Grains of altered granite and mylonite were also identified in this size section. Grains of quartz, fluorite and sulphides precipitated as a result of hydrothermal circulation are frequent. Idiomorphic crystal growth indicates open pore spaces.

5 Model C. Tunnel Chainage 2/163 m

The zone identified at this site intersects the tunnel ceiling at chainage 2/163 m. The structure interpreted before drilling strikes SE 139° and dips SW 79° /Stigsson et al. 2003/. Based on tunnel observation the zone can be characterized as a single fracture rather than a fault, with addition of some local sections of crushed rock. There are no brittle splay structures, and no signs of displacement, see Appendix 4 for a detailed geological map of the tunnel wall.

Four holes, KA2169A01, KA2169A02, KA2169A03 and KA2169A04, were drilled from the tunnel in the proximity of the identified structure (Figure 5-1). The rock identified in the boreholes is granodiorite (Äspö Diorite) with occasional aplite and granite, see Appendix 3. The RQD varies between 81 and 99.

Crushed rock and subordinate breccia occur with widths of 1-5 cm in the 4 holes, at L=2.5 m in KA2169A01, at L=3 m in KA2169A02, at L=3.95 m in KA2169A03, and at L=2.87 m in KA2169A04, see Figure 5-1. The material is flaky, sub-zones are less than 1 cm wide. Minerals in the zone appear to be minerals of the wall rock. The sub-zones occur in good quality rock and do not influence on RQD at all. The structures identified in KA2169A01 to KA2169A03 appear aligned and their orientations determined from BIPS logging fit well to the orientation of the zone in the tunnel. Their indications are found somewhat deeper than expected from the previously modeled structure. The intercept identified in KA2169A04 is much closer to the casing than the depth of intersection predicted from the modeled structure. Furthermore the orientation of the intercept identified in KA2169A04 does not fit very well with zone 2163. Hence this structure is considered to be a single fracture. Two other single fractures are identified in KA2169A01 and KA2169A02 (Figure 5-1).

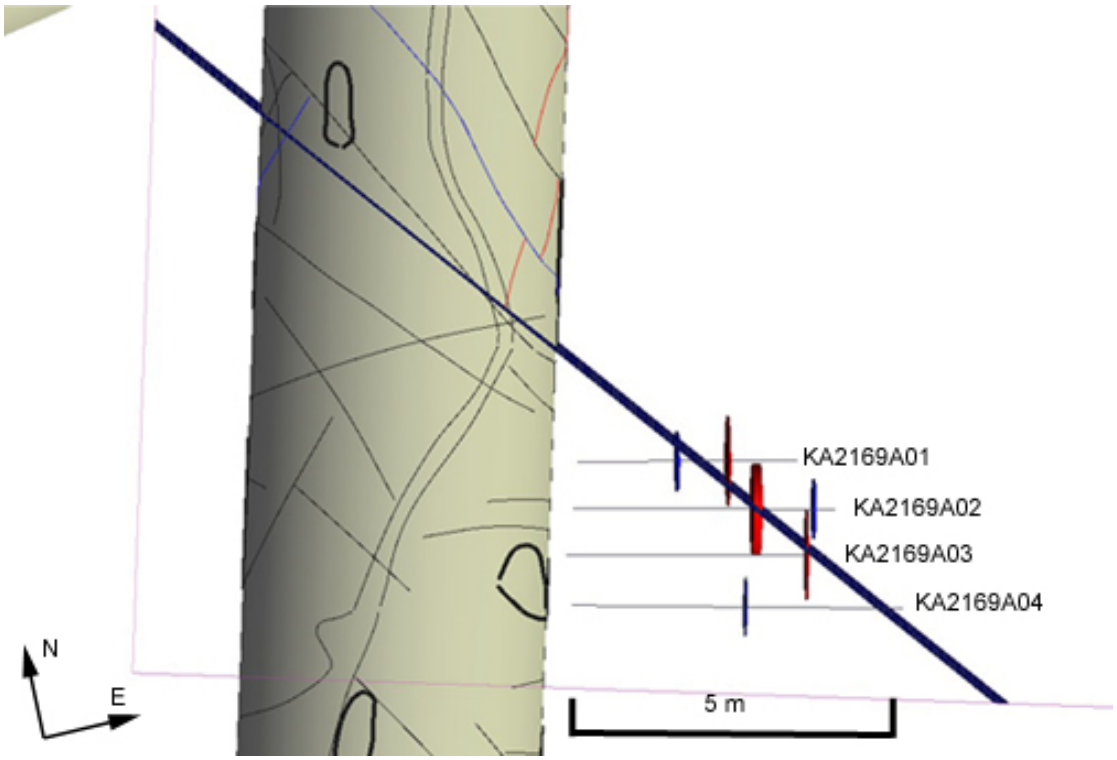

Figure 5-1. *RVS model C with borehole and fault geometry. The red discs are indications of 'zone 2163'. The smaller blue discs are indications of zones not associated with the main structure.*

No water flow was observed in any of the boreholes during drilling. Water flows between 235 and 250 ml/min were measured after completion of drilling in boreholes KA2169A01 to KA2169A03. Similar water flows in these three holes indicate that these intercepts belong to the same water-bearing structure. The borehole KA2169A04 is dry during and after drilling.

The structure has been remodeled on the basis of tunnel survey and the mapped occurrences in the boreholes (Figure 5-2). The deviation of the geometry of the updated structure compared to the one based on the original model is minor and the updated orientation is 308.7 / 85.5.°

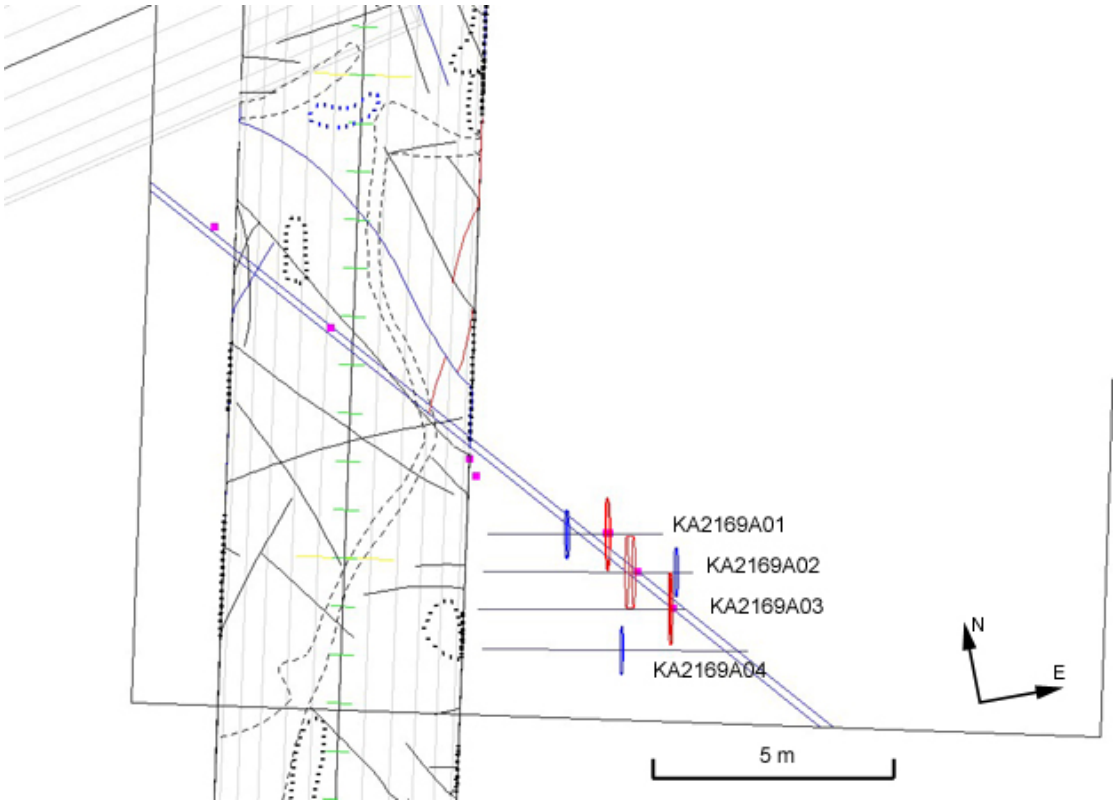

Figure 5-2. *Illustration of the points (purple) in the tunnel and in the boreholes used for remodeling the 'zone 2163'.*

The zone is identified as a NW trending structure in quartz monzodiorite running parallel with a set of thin epidote sealed fractures (possibly very thin mylonites?). The zone contains fault crush as well as fault gouge at least in boreholes KA2169A02 and KA2169A03, and to some extent in KA2169A01. The zone is widest in borehole KA2169A02 (ca 15 cm of crush and gouge). The absence of water flow in KA2169A04 confirms the judgment that the structure is more likely a single fracture. The absence of 'zone 2163' in this borehole might be an indication that the zone gradually bends to the east.

The zone is regarded as being suitable for resin injection in crush rock in holes KA2169A01 to KA2169A03. The crush may be due to tensile cracking as a response to a two dimensional stress in the fracture plane, more than to shear.

From the sampling of the zone in borehole KA2169A02 the following "grain size distribution" is defined (total weight of sample 450 g): larger than 2 mm, 434g; 1-2 mm, 8 g; 0.25 mm-0.5 mm, 2g; 0.125mm-0.25 mm, 1g and <0.125 mm, 5 g. The largest portion of the material consists of rock fragments whereas the fine material constitutes a minor part. Macroscopical observations of the 1-2 mm fraction show the presence of grains of altered quartz monzodiorite and epidote-rich fine-grained (mylonitic?) grains. A few grains containing idiomorphic calcite crystals in the order of 50-100 μm indicate growth of these crystals in open pore spaces.

6 Model D. Tunnel Chainage 1/600 m

This zone intersects the tunnel crest line at chainage 1/600 m. The structure as interpreted prior to drilling strikes NE 44° and dips NW 85° /Stigsson et al. 2003/. Its width varies from 40 to 50 cm, and the material can be characterized as a chlorite phyllonite, probably an altered and mechanically degraded (mylonitized) amphibolite dyke. It contains 5-10 cm wide sub-zones of chloritic fault gouge with some rock fragments, see Appendix 4.

The accurate survey made in conjunction with the experiment show discrepancy in the position of zone occurrences in the tunnel. The ‘zone 1600’ therefore has been remodeled. The points used for reinterpretation are illustrated in Figure 6-1. The remodeled structure strikes 28° and dips 75°.

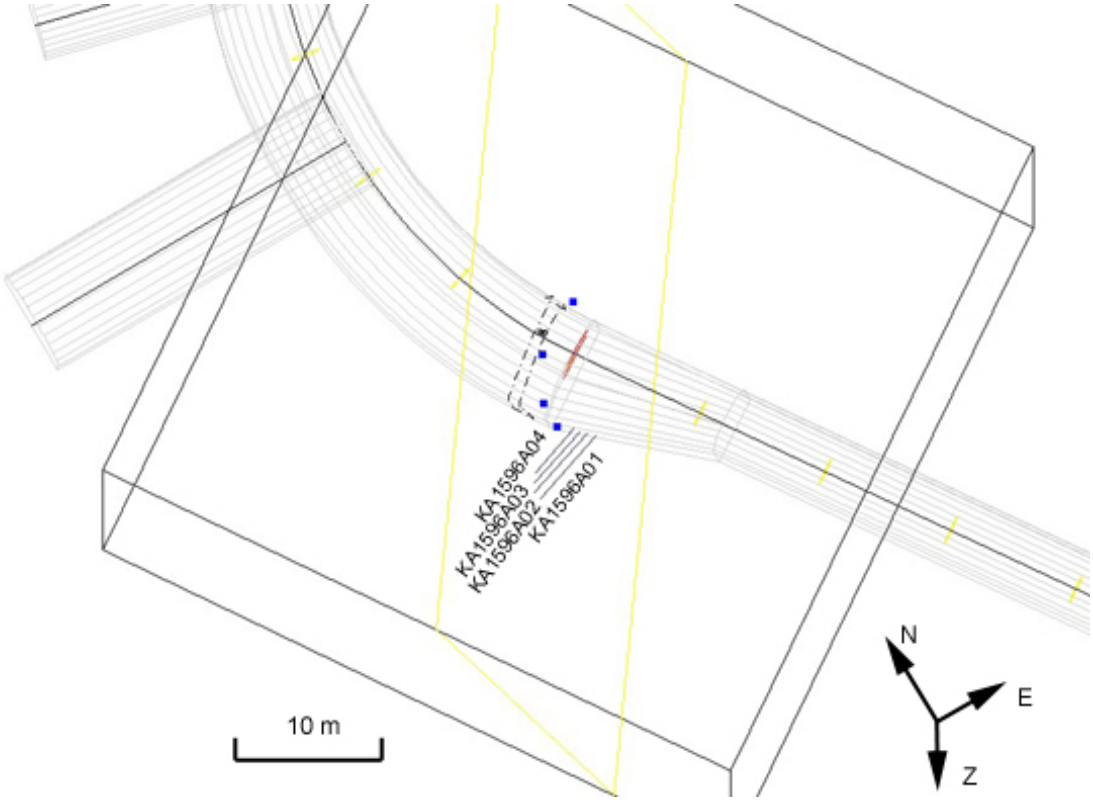

Figure 6-1. *Visualization of the points (blue) based on tunnel survey and used for the remodeling of ‘zone 1600’, and positions of the boreholes.*

Four boreholes; KA1596A01, KA1596A02, KA1596A03 and KA1596A04 were drilled from the tunnel in the vicinity of the interpreted structure (Figure 6-1). The rock in the boreholes is mainly granodiorite (Äspö Diorite) with subordinate chloritic phyllonite , fine grained, red protocataclastic granite, and minor occurrences of pegmatite, see Appendix 3. RQD varies between 75 (where the zone occurs) and 100.

The structure occurs in all four boreholes, at L=5.55 m in KA1596A01, at L=4.7 m in KA1596A02, at L=3.3 m and L=4.2 m in KA1596A03, and at L=2.55 m in KA1596A04 (Figure 6-2). The thickness of the zone varies from 10 cm to 40 cm and the zone is divided into two branches inboreholeKA1596A03.

The occurrences of ’zone 1600’ in the drill cores fit fairly well with tunnel observations and with orientations indicated by BIPS logging, see Figure 6-2. The fault gouge contains clay minerals, mainly chlorite and rock fragments.

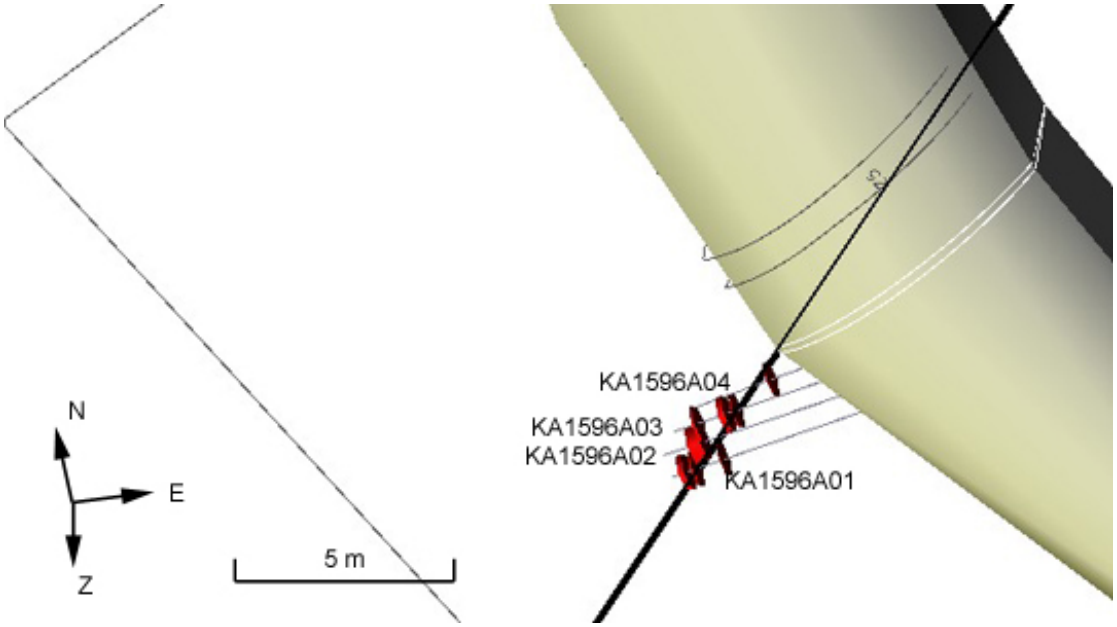

Figure 6-2. *Location of zone occurrences in the boreholes associated with ‘zone 1600’ as modeled from tunnel observations.*

No water flow was observed during drilling in boreholes KA1596A02 to KA1596A04. Some water flow was measured in the last meter of drilling of borehole KA1596A01. Water flow after the completion of drilling shows significant variability between the boreholes: 600 ml/min were measured in KA1596A01, 4 ml/min in KA1596A03, and no flow in KA1596A02 and KA1596A04, suggesting significant heterogeneity.

This structure occurs in various rock types, such as chloritic phyllonite, pegmatite and granite. When sheared, these rocks have been deformed in different ways. Chloritic phyllite has undergone ductile (plastic) deformation (to a phyllonite) and is practically tight, as can be seen on tunnel wall A (outer) and in boreholes KA1596A02-A04 (see appendix 1). The brittle granite and pegmatite have been crushed and is highly water bearing, as can be seen on tunnel wall B (inner) and in borehole KA1596A01.

The structure can be characterized as a normal fault, considering how some splay cracks are bent, but no magnitude of displacement can be determined. The structure is partly water bearing, especially where fault gouge is encountered in borehole KA1596A01. The zone is not one single zone but diverges and converges in width. In borehole KA1596A01 the gouge is coarser, and the borehole carried water (after drilling through the structure, while the other holes were almost entirely dry, 0-4 ml/min.

That part seems to be crushed portions of pegmatite and the host rock, while the other holes intersect the zone where in amphibolite, which is altered and mechanically deformed to chlorite phyllonite.

The zone is regarded as being suitable for resin injection experiments in fault gouge.

This is the widest of the 4 investigated zones, in the order of 40 to 50 cm wide. It consists of extremely chlorite/clay mineral rich material on both sides of a quartz pegmatite (1-2 dm wide). The zone shows almost the same appearance in all four boreholes but some variations can be noticed. For example a chlorite/clay rich 5 cm thick branch is found in borehole KA1596A04 about half a metre away from the main structure. It is also obvious that the thickness of the quartz-pegmatite varies significantly.

The part of the structure at chainage 1/600 m interesting for the resin injection experiment is the c. 2 dm wide chlorite/clay-rich section found in the inner part of the boreholes (beyond the quartz-pegmatite). From macroscopical observations of sieved material from this zone it is obvious that also the larger pieces (0.5 to 2 mm) are very rich in chlorite/clay minerals although some grains containing quartz and K-feldspar were also observed. A complete siewing was not possible due to the clayrich material in this zone. XRD identification of the clay minerals suggest existence of mixed layer clays (probably chlorite/smectite-vermiculite or corrensite) are important constituents in the fine grained fraction, cf. Appendix 6.

7 Mineralogy and geochemistry

Table 7-1 shows the samples collected for mineralogical identification and sorption experiments on fault gouge material. Samples have been analysed in thin section, ICP and XRD. Preliminary results from laboratory tests are presented in Appendices 5 and 6.

Table 7-1. List of samples for mineralogical identification and determination of K_d of fault gouge material collected from the experimental boreholes.

Borehole ID	Borehole intercept (metres)	Description sample and planned analyses
KA 1596A01	5.40-5.65	Piece of fault rock and 1-2 mm fragments for thin sections <0.125 mm fraction for XRD and ICP analyses.
KA 2169A01	2.47-2.70	Spare sample (can be used for additional analyses or laboratory tests
KA 2169A02	: 2.70-2.85	Piece of fault rock and 1-2 mm fragments for thin sections <0.125 mm fraction for XRD and ICP analyses.
KA 2423A01	4.22-4.30	Spare sample (can be used for additional analyses or laboratory tests
KA 2423A02	2.70-2.75	Spare sample (can be used for additional analyses or laboratory tests
KA 2423A03	2.36-2.53	Piece of fault rock and 1-2 mm fragments for thin sections <0.125 mm fraction for XRD and ICP analyses.

8 Conclusions

- Model A, ‘zone 2545’: Some of the fractures cut by the core drillings are regarded as being typical for the NW striking fracture set. BIPS logs have confirmed that this is the case. The fractures carry water. However, as the zone does not contain any loose material, it is not within the scope of the present characterization project. Furthermore none of the fractures have been cut by more than one borehole. Therefore none of the holes are recommended for epoxy resin injection.

- Model B, ‘zone 2430’: Fault breccia and subordinate fault crush with a width of one or two cm has been observed in all boreholes. However the zone appears to yield very little water.

- Model C, ‘zone 2163’: Three of the boreholes have encountered a water-bearing fracture. The fourth has intercepted a narrow zone with fault crush, but showing no water. The water-bearing zone appears to be typical of the NW striking set of water-bearing fracture swarms. Fault crush and subordinate fault breccia occur in three of the holes.

- Model D, ‘zone 1600’: This structure is set in different rock types such as chloritic phyllite, pegmatite and granite. When sheared, these rocks have been deformed in different ways. Chloritic phyllite has undergone ductile (plastic) deformation and is practically tight, as can be seen on tunnel wall A (outer) and in holes KA1596A02-A04. The brittle granite and pegmatite have been crushed and is highly water bearing, as can be seen on tunnel wall B (inner) and in hole KA1596A01. Fault gouge and subordinate fault breccia occur.

- Some of the zones contain material of a loose type with low clay content. These tend to disintegrate, and the drill cores have been protected with plastic foil, but several have been deformed by the drilling prcess. The epoxy resin may stabilize and preserve these structures, if carried out carefully. It should be possible to obtain a more complete picture of the structures in overcored samples, for which reason it is recommended to thoroughly map the structures.

- The two NE striking zones 1/600 and 2/430 are certified master faults. At both locations, sub-horizontal splay faults are identified, indicating a sub-vertical displacement direction, appearing to be of a normal fault type. There are no structures to identify the magnitude of displacement. No vertical splay cracks could be identified.

- No certified faulting could be identified along the two NW striking zones, and no certain splay cracks were identified there. InboreholeKA2549A01 a NE striking master fault was identified. A number of joints appearing to be NW oriented, appear to terminate towards the NE structure.

- Cores which may be suitable for epoxy resin injection are listed in Table 8-1, with location of target zones and tentative packer position for each hole.

- The evaluation of the drill cores from the four structures at chainages 1/600 m, 2/163 m, 2/430 m and 2/545 m support the suitability of three structures (at 1/600 m, 2/163 m and 2/430 m) for epoxy resin injections. The ‘zone 2545’, in contrast, show a more complex geometry and it is recommended not to include this structure in the resin injection experiments. Therefore no mineralogical sampling and analysis is carried on material from this structure.

Table 8-1. Boreholes suitable for epoxy resin injection with interpreted depths of target zones and tentative positions of mechanical packer for each borehole.

Borehole ID	Target zone (metres)	Zone position (metres)	Recommended packer position (metres from tunnel rock surface)
KA1596A01	1600 (Model D)	5.48-5.62	5
KA1596A02	1600 (Model D)	4.5-4.84	3.45
KA1596A03	1600 (Model D)	3.14-3.52; 4.15-4.22	2.65
KA1596A04	1600 (Model D)	2.32-2.80	1.1
KA2169A01	2163 (Model C)	2.47-2.49	1.9
KA2169A02	2163 (Model C)	2.96-3.10	2.6
KA2169A03	2163 (Model C)	3.95-3.98	3.5
KA2169A04	No zone found	-	None
KA2423A01	2430 (Model B)	4.22-4.26	3.5
KA2423A02	2430 (Model B)	2.72-2.75	2.2
KA2423A03	2430 (Model B)	2.36-2.53	1.8
KA2423A04	2430 (Model B)	1.92-1.94	1.3
KA2548A01	Zone not found	1.58-1.62	None
KA2549A01	Zone not found	2.02-2.15	None
KA2549A02	Zone not found	-	None
KA2549A03	Zone not found	-	None

9 References

Birgersson L 2002. TRUE-1 Continuation Project. Characterization of fault rock zones using epoxy resin injection. Unpublished Project Plan, dated 2002-12-19.

Mazurek M, Bossart P and T Eliasson 1996. Classification and characterization of water-conducting features at Äspö: Results of investigations on the outcrop scale. SKB ICR 97-01.

Stigsson M, Hermanson J and O Forsberg 2003. TRUE-1 Continuation Project. Fault rock zones. Structural models of tentative experiment sites. Äspö Hard Rock Laboratory, International Progress Report IPR-03-49

Appendix 1. Photographs of tunnel sections and cores from each candidate site

Figure A1-1. *KA2549A01, core details at 2.31 m.*

Figure A1-2. *KA2424A02 drill core.*

Figure A1-3. *Fault at 2.5 m in KA2424A02 drill core.*

Figure A1-4. *Fault visible in tunnel section 2/430 m.*

Figure A1-5. *Drill core of KA2169A04.*

Figure A1-6. *Fault in KA2169A04 at 3 m borehole length.*

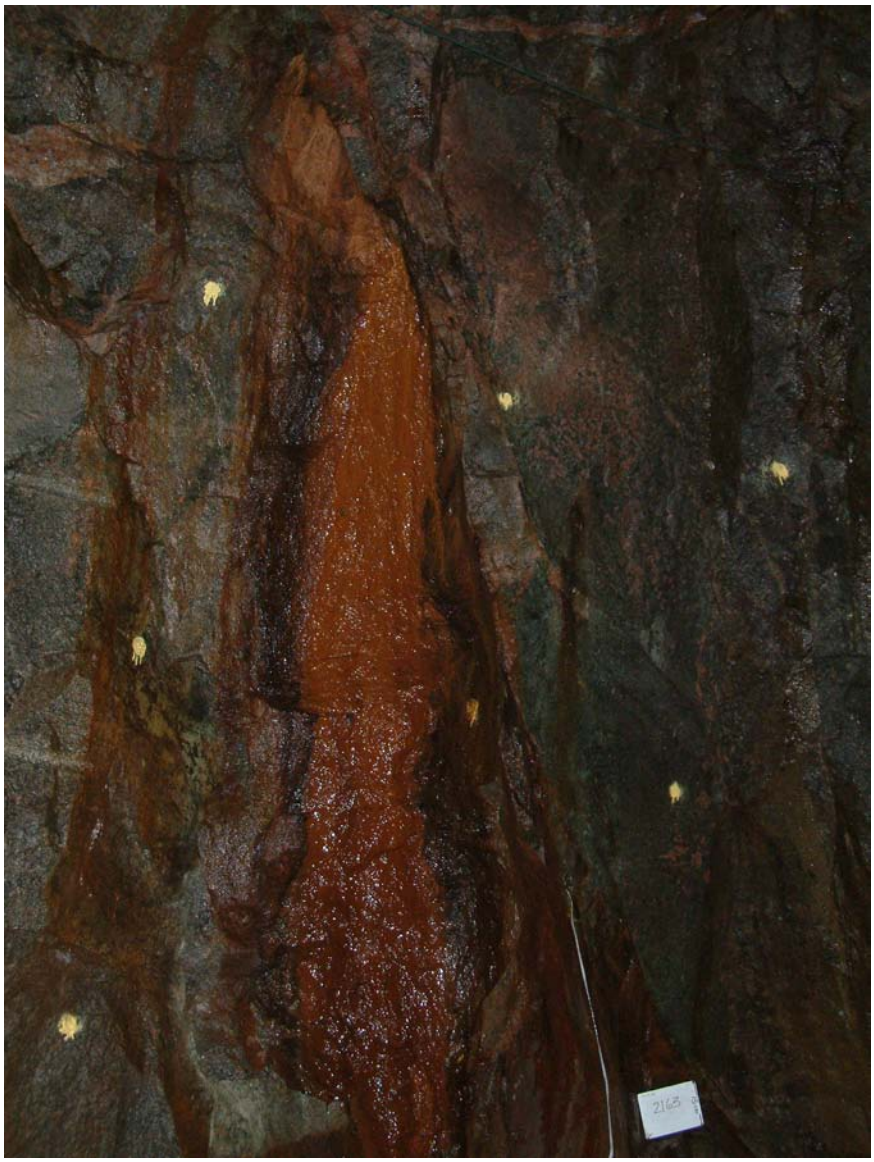

Figure A1-7. *Fault in tunnel section 2/163 m.*

Figure A1-8. *Drill core of KA1596A02.*

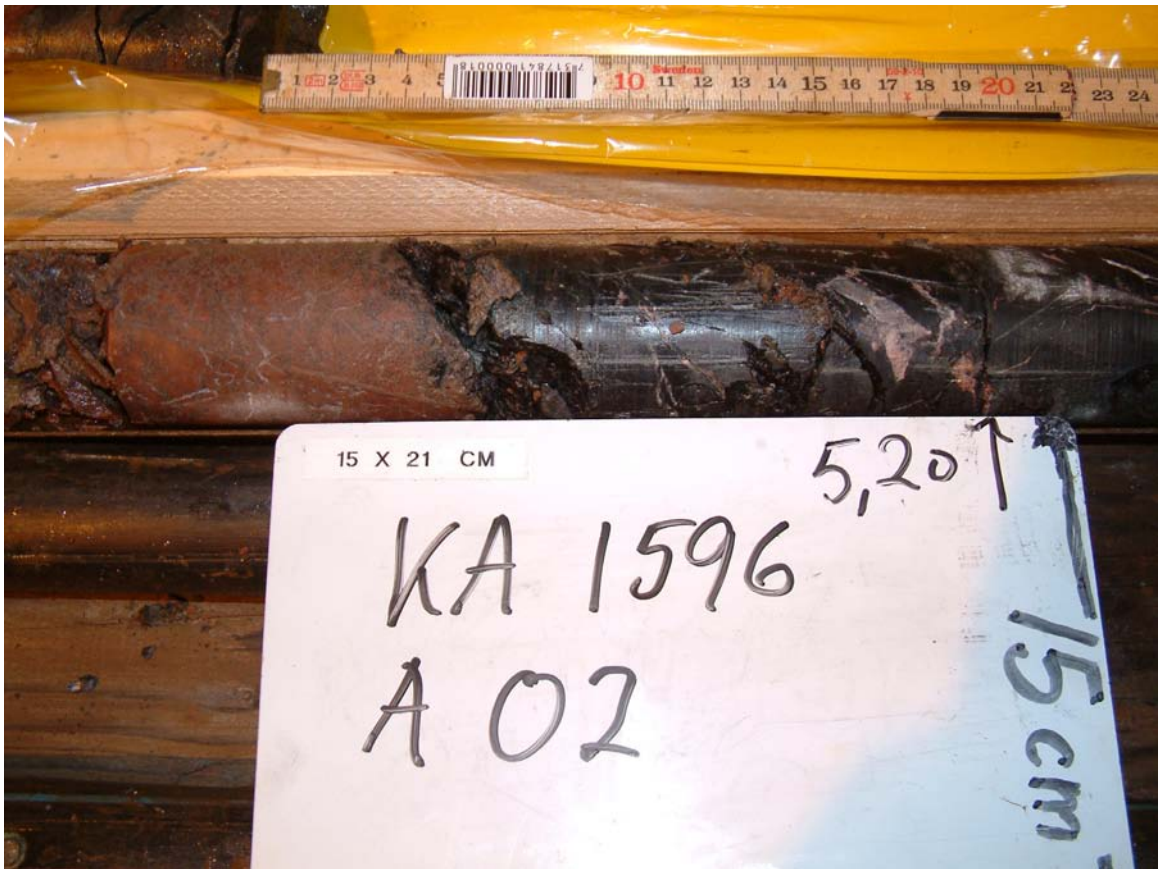

Figure A1-9. *Detail of fault at 5.2 m borehole depth in KA1596A02.*

Figure A1-10. *Target fault zone at tunnel section 1/600 m.*

Figure A1-11. *Detail of target fault zone at tunnel section 1/600 m.*

Appendix 2: Detailed tabulations of findings in each of the drilled boreholes

A2a: Geometrical borehole data

IDCODE	STARTDATE	STOPDATE	Äspö 96 EASTING	Äspö 96 NORTHING	Äspö 96 ELEVATION	Äspö 96 BEARING	INCLINATION	BHLEN, m	RT 90 BEARING
KA1596A01	2003-03-31	2003-03-31	7227,795	2032,284	-219,815	255,791	-4,67766	5,94	244
KA1596A02	2003-03-31	2003-03-31	7228,269	2031,872	-219,89	256,251	-4,66443	5,62	244
KA1596A03	2003-03-31	2003-03-31	7228,686	2031,467	-219,988	256,0595	-4,58199	4,8	244
KA1596A04	2003-03-31	2003-03-31	7229,147	2031,239	-220,063	254,7771	-4,47867	4,1	243
KA2169A01	2003-04-08	2003-04-08	2308,286	7214,797	-290,891	101,5268	-3,63168	3,62	90
KA2169A02	2003-04-08	2003-04-08	2308,043	7214,054	-290,632	101,905	-3,01311	4,32	90
KA2169A03	2003-04-08	2003-04-08	2307,785	7213,325	-290,705	101,7565	-2,26251	4,28	90
KA2169A04	2003-04-08	2003-04-08	2307,695	7212,498	-290,934	102,3693	-3,45735	5,47	90
KA2423A01	2003-03-25	2003-03-25	7154,467	2093,143	-322,666	209,3018	-3,10959	5,04	197
KA2423A02	2003-03-25	2003-03-25	7154,869	2092,521	-322,788	215,603	-3,68685	3,72	204
KA2423A03	2003-03-25	2003-03-25	7155,358	2092,223	-322,861	218,2591	-4,3209	2,93	206
KA2423A04	2003-03-25	2003-03-25	7155,751	2091,842	-322,939	222,598	-4,4343	3,11	211
KA2548A01	2003-04-07	2003-04-07	7255,754	2021,377	-338,569	278,0134	-3,78738	4,64	266
KA2549A01	2003-04-07	2003-04-07	7256,701	2022,036	-338,657	275,9266	-3,71943	3,69	264
KA2549A02	2003-04-07	2003-04-07	7257,22	2022,205	-338,727	277,7223	-3,74796	5,21	266
KA2549A03	2003-04-07	2003-04-07	7257,791	2022,378	-338,785	281,2744	-3,39858	5,57	269
Total length								**72,06**	

A2b: Rock types

Site	Hole ID	Secup	Seclow	Rock type	Description
Äspö	KA1596A01	0,00	3,50	diorite	porphyroblastic, dark grey granodiorite-diorite
Äspö	KA1596A01	3,50	3,60	granite	cataclasite
Äspö	KA1596A01	3,50	5,45	pegmatite	protocataclastic
Äspö	KA1596A01	3,60	5,25	diorite	porphyroblastic, dark grey granodiorite-diorite
Äspö	KA1596A01	5,45	5,60	fault breccia	50% matrix
Äspö	KA1596A01	5,60	5,94	red granite	protocataclastic
Äspö	KA1596A02	0,00	4,40	diorite	porphyroblastic, dark grey granodiorite-diorite
Äspö	KA1596A02	4,40	4,52	pegmatite	
Äspö	KA1596A02	4,52	4,85	chloritic phyllite	fault gouge
Äspö	KA1596A02	4,85	5,20	red granite	protocataclastic
Äspö	KA1596A02	5,20	5,62	chloritic phyllite	
Äspö	KA1596A03	0,00	2,05	diorite	porphyroblastic, dark grey granodiorite-diorite
Äspö	KA1596A03	2,05	2,30	pegmatite	
Äspö	KA1596A03	2,30	2,40	ultracataclasite	
Äspö	KA1596A03	2,40	2,55	cataclasite	
Äspö	KA1596A03	2,55	3,15	Protocataclasite	
Äspö	KA1596A03	3,15	4,10	pegmatite	
Äspö	KA1596A03	4,10	4,30	chloritic phyllite	gouge
Äspö	KA1596A03	4,30	4,80	diorite	porphyroblastic, dark grey granodiorite-diorite
Äspö	KA1596A04	0,00	2,90	diorite	porphyroblastic, dark grey granodiorite-diorite
Äspö	KA1596A04	2,90	3,60	red granite	protocataclastic
Äspö	KA1596A04	3,60	4,04	mylonite	
Äspö	KA2169A01	0,00	3,62	granodiorite	medium grain non-porphyroblastic, dark grey granodiorite
Äspö	KA2169A02	0,00	4,32	granodiorite	medium grain non-porphyroblastic, dark grey granodiorite. Irregular pegmatite at 1.80
Äspö	KA2169A03	0,00	4,28	granodiorite	medium grain non-porphyroblastic, dark grey granodiorite. Aplite vein 1-2 cm at 1.08
Äspö	KA2169A04	0,00	5,47	granodiorite	medium to coarse grain non-porphyroblastic, grey granodiorite with occasional granitic layers
Äspö	KA2423A01	0,00	3,93	Granite	light grey, medium grain, biotite granite
Äspö	KA2423A01	3,93	4,35	Protocataclasite	matrix 15%, 1-2 cm clasts
Äspö	KA2423A01	4,35	5,04	diorite	porphyroblastic, dark grey granodiorite-diorite
Äspö	KA2423A02	0,00	1,55	Granite	light grey, medium grain, biotite granite
Äspö	KA2423A02	1,55	1,65	Aplite	
Äspö	KA2423A02	1,65	3,72	Granite	light grey, medium grain, biotite granite
Äspö	KA2423A03	0,00	2,93	Granite	light grey, medium grain, biotite granite
Äspö	KA2423A04	0,00	3,11	Granodiorite	
Äspö	KA2549A01	0,00	3,69	red granite	red medium grain, slightly gneissic granite w porphyroblasts
Äspö	KA2549A02	0,00	1,60	granodiorite	medium to coarse grain porphyroblastic, grey granodiorite
Äspö	KA2549A02	3,05	3,80	Protocataclasite	source rock: granodiorite
Äspö	KA2549A02	3,80	5,21	granodiorite	medium to coarse grain porphyroblastic, grey granodiorite
Äspö	KA2549A03	0,00	2,10	granodiorite	medium to coarse grain porphyroblastic, grey granodiorite
Äspö	KA2549A03	1,60	1,90	Pegmatite	
Äspö	KA2549A03	2,10	4,35	granite	red, acid, medium grain with xenoliths of diorite
Äspö	KA2549A03	4,35	5,50	granodiorite	medium to coarse grain porphyroblastic, grey granodiorite
Äspö	KA2548A01	0,00	0,35	granodiorite	medium to coarse grain porphyroblastic, grey granodiorite
Äspö	KA2548A01	0,35	0,45	aplite	
Äspö	KA2548A01	0,45	0,70	granodiorite	medium to coarse grain porphyroblastic, grey granodiorite
Äspö	KA2548A01	0,70	2,10	granite	red, acid, medium grain with xenoliths of diorite
Äspö	KA2548A01	1,90	3,05	granodiorite	medium to coarse grain porphyroblastic, grey granodiorite
Äspö	KA2548A01	2,10	4,65	granodiorite	medium to coarse grain porphyroblastic, grey granodiorite

A2c: Fracture mapping

Site	Hole ID	Depth	Angle vs hole axis	Quantity	Remark
Äspö	KA1596A01	0,30	60	1	
Äspö	KA1596A01	0,30	90	1	
Äspö	KA1596A01	0,35	30	1	
Äspö	KA1596A01	0,35	70	1	
Äspö	KA1596A01	0,60	90	1	
Äspö	KA1596A01	0,95	55	2	mylonite 60 degrees
Äspö	KA1596A01	1,15	20	1	mylonite, 1 mm
Äspö	KA1596A01	1,26	30	1	
Äspö	KA1596A01	1,30	30	1	mylonite 1 mm
Äspö	KA1596A01	1,67	60	1	
Äspö	KA1596A01	1,77	60	1	parallel w 1.67
Äspö	KA1596A01	2,50	60	1	mylonite & cataclasite 8 mm
Äspö	KA1596A01	2,54	30	1	
Äspö	KA1596A01	2,60	20	1	
Äspö	KA1596A01	3,10	70	1	
Äspö	KA1596A01	3,18	35	1	
Äspö	KA1596A01	3,26	30	1	
Äspö	KA1596A01	3,36	70	2	
Äspö	KA1596A01	3,60	60	1	mylonite
Äspö	KA1596A01	3,90	60	2	
Äspö	KA1596A01	4,05	90	2	
Äspö	KA1596A01	4,20	20	1	
Äspö	KA1596A01	4,25	20	1	
Äspö	KA1596A01	4,36	80	1	
Äspö	KA1596A01	4,50	35	1	
Äspö	KA1596A01	4,58	30	1	
Äspö	KA1596A01	4,62	70	1	
Äspö	KA1596A01	4,75	70	1	
Äspö	KA1596A02	0,10	50	1	
Äspö	KA1596A02	0,20	60	2	
Äspö	KA1596A02	0,30	80	2	
Äspö	KA1596A02	0,51	60	1	
Äspö	KA1596A02	0,85	40	1	
Äspö	KA1596A02	0,95	40	1	
Äspö	KA1596A02	1,10	60	1	
Äspö	KA1596A02	1,20	80	1	
Äspö	KA1596A02	1,75	60	1	
Äspö	KA1596A02	1,85	60	1	
Äspö	KA1596A02	1,95	60	1	
Äspö	KA1596A02	2,05	90	1	
Äspö	KA1596A02	2,15	90	1	
Äspö	KA1596A02	2,37	60	1	
Äspö	KA1596A02	2,66	45	1	
Äspö	KA1596A02	3,12	90	1	
Äspö	KA1596A02	3,13	45	1	
Äspö	KA1596A02	3,40	30	1	
Äspö	KA1596A02	3,85	50	1	
Äspö	KA1596A02	3,95	60	1	
Äspö	KA1596A02	4,12	65	1	
Äspö	KA1596A02	4,20	90	2	
Äspö	KA1596A02	4,37	50	1	
Äspö	KA1596A02	4,50	40	1	
Äspö	KA1596A02	4,65	40	1	
Äspö	KA1596A02	4,78	40	1	
Äspö	KA1596A02	4,90	50	1	
Äspö	KA1596A02	5,00	50	1	
Äspö	KA1596A02	5,10	50	1	
Äspö	KA1596A02	5,30	50	1	
Äspö	KA1596A03	0,05	70	1	
Äspö	KA1596A03	0,25	60	2	
Äspö	KA1596A03	0,25	30	1	
Äspö	KA1596A03	0,75	30	1	
Äspö	KA1596A03	0,75	60	1	

A2c: Fracture mapping, continued

Site	Hole ID	Depth	Angle vs hole axis	Quantity	Remark
Äspö	KA1596A03	0,98	35	1	
Äspö	KA1596A03	1,03	60	1	
Äspö	KA1596A03	1,61	70	1	
Äspö	KA1596A03	1,70	37	1	
Äspö	KA1596A03	1,88	60	1	
Äspö	KA1596A03	2,12	60	1	
Äspö	KA1596A03	2,19	90	1	
Äspö	KA1596A03	2,25	45	1	
Äspö	KA1596A03	2,25	60	2	
Äspö	KA1596A03	2,52	60	1	
Äspö	KA1596A03	2,90	80	1	
Äspö	KA1596A03	3,05	30	1	
Äspö	KA1596A03	3,05	60	1	
Äspö	KA1596A04	0,05	90	2	
Äspö	KA1596A04	0,10	20	1	
Äspö	KA1596A04	0,15	90	1	
Äspö	KA1596A04	0,70	10	1	
Äspö	KA1596A04	0,85	63	1	
Äspö	KA1596A04	1,15	35	1	
Äspö	KA1596A04	1,55	60	1	
Äspö	KA1596A04	1,65	70	2	
Äspö	KA1596A04	1,80	60	1	
Äspö	KA1596A04	1,90	30	1	
Äspö	KA1596A04	3,10	50	1	
Äspö	KA1596A04	3,20	80	1	
Äspö	KA1596A04	3,30	70	1	
Äspö	KA1596A04	3,60	70	1	

A2c: Fracture mapping, continued

Site	Hole ID	Depth	Angle vs hole axis	Quantity	Remark
Äspö	KA2169A01	0,30	80	1	no visible minerals, slight surface stain
Äspö	KA2169A01	0,40	15	1	chlorite, some crush width 1 mm
Äspö	KA2169A01	0,55	50	1	no visible minerals, slight surface stain
Äspö	KA2169A01	0,60	30	1	chlorite, some crush width <1 mm
Äspö	KA2169A01	0,74	90	1	no visible minerals, slight surface stain
Äspö	KA2169A01	1,29	60	1	clay min width<1mm
Äspö	KA2169A01	1,47	30	1	no visible minerals, slight surface stain
Äspö	KA2169A01	1,85	35	1	no visible minerals, slight surface stain
Äspö	KA2169A01	2,12	75	1	no visible minerals, slight surface stain
Äspö	KA2169A01	2,18	75	1	no visible minerals, slight surface stain
Äspö	KA2169A01	2,22	50	1	no visible minerals, slight surface stain
Äspö	KA2169A01	2,49	35	1	no visible minerals, slight surface stain
Äspö	KA2169A01	2,73	30	1	no visible minerals, slight surface stain
Äspö	KA2169A01	2,90	90	1	no visible minerals, slight surface stain
Äspö	KA2169A01	3,00	40	1	no visible minerals, slight surface stain
Äspö	KA2169A02	0,20	60	1	no visible minerals, slight surface stain
Äspö	KA2169A02	1,00	10	1	no visible minerals, slight surface stain
Äspö	KA2169A02	1,81	50	1	no visible minerals, slight surface stain
Äspö	KA2169A02	1,88	80	1	no visible minerals, slight surface stain
Äspö	KA2169A02	1,90	50	1	no visible minerals, slight surface stain
Äspö	KA2169A02	2,41	65	1	no visible minerals, slight surface stain
Äspö	KA2169A02	3,38	80	1	no visible minerals, slight surface stain
Äspö	KA2169A02	3,92	40	1	no visible minerals, slight surface stain
Äspö	KA2169A02	4,26	25	1	no visible minerals, slight surface stain
Äspö	KA2169A03	0,10	80	1	no visible minerals, slight surface stain
Äspö	KA2169A03	0,20	40	1	chlorite coating, illite
Äspö	KA2169A03	0,28	50	1	no visible minerals, slight surface stain
Äspö	KA2169A03	0,75	25	1	thin chlorite coating
Äspö	KA2169A03	1,02	30	1	no visible minerals, slight surface stain
Äspö	KA2169A03	1,45	40	1	no visible minerals, slight surface stain
Äspö	KA2169A03	1,72	60	1	no visible minerals, slight surface stain
Äspö	KA2169A03	2,09	50	1	no visible minerals, slight surface stain
Äspö	KA2169A03	2,18	50	1	no visible minerals, slight surface stain
Äspö	KA2169A03	2,30	70	1	no visible minerals, slight surface stain
Äspö	KA2169A03	3,18	35	1	no visible minerals, slight surface stain
Äspö	KA2169A03	3,95	30	1	no visible minerals, slight surface stain
Äspö	KA2169A03	4,22	55	1	no visible minerals, slight surface stain
Äspö	KA2169A04	0,05	70	1	no visible minerals, slight surface stain
Äspö	KA2169A04	0,26	70	1	no visible minerals, slight surface stain
Äspö	KA2169A04	0,56	50	1	no visible minerals, slight surface stain
Äspö	KA2169A04	0,77	60	1	sub-parallel to 0.56. no visible minerals, slight surface stain
Äspö	KA2169A04	1,31	50	1	high angle to 0.77. no visible minerals, slight surface stain
Äspö	KA2169A04	2,13	50	1	parallel to 1.31. no visible minerals, slight surface stain
Äspö	KA2169A04	3,56	20	1	thin illite coating
Äspö	KA2169A04	3,71	45	1	calcite < 1 mm

A2c Fracture mapping, continued

Site	Hole ID	Depth	Angle vs hole axis	Quantity	Remark
Äspö	KA2423A01	0,20	45	1	illite
Äspö	KA2423A01	0,22	75	1	mylonite
Äspö	KA2423A01	0,27	70	1	
Äspö	KA2423A01	0,45	75	1	
Äspö	KA2423A01	0,55	65	1	
Äspö	KA2423A01	0,60	55	1	
Äspö	KA2423A01	1,00	30	1	illite
Äspö	KA2423A01	2,69	90	1	
Äspö	KA2423A01	3,93	70	1	
Äspö	KA2423A01	4,05	45	1	
Äspö	KA2423A01	4,35	45	1	10 cm fault breccia. Loose 1-2 cm clasts in 15% matrix
Äspö	KA2423A02	0,08	20	1	
Äspö	KA2423A02	0,14	60	1	
Äspö	KA2423A02	0,19	50	1	
Äspö	KA2423A02	0,27	65	1	
Äspö	KA2423A02	0,56	40	1	
Äspö	KA2423A02	1,60	30	1	
Äspö	KA2423A02	2,70	90	1	
Äspö	KA2423A02	2,75	45	1	
Äspö	KA2423A02	2,92	90	1	
Äspö	KA2423A02	3,30	90	1	
Äspö	KA2423A02	4,47	45	1	
Äspö	KA2423A03	0,03	80	1	
Äspö	KA2423A03	0,22	70	1	
Äspö	KA2423A03	1,43	90	1	
Äspö	KA2423A03	2,20	30	1	
Äspö	KA2423A03	2,42	50	1	
Äspö	KA2423A03	2,48	50	1	
Äspö	KA2423A03	2,55	30	1	
Äspö	KA2423A03	2,56	40	1	
Äspö	KA2423A03	2,57	60	1	
Äspö	KA2423A04	0,07	70	1	
Äspö	KA2423A04	0,35	85	1	
Äspö	KA2423A04	0,46	80	1	
Äspö	KA2423A04	1,35	20	1	
Äspö	KA2423A04	1,50	30	1	
Äspö	KA2423A04	2,26	25	1	green mylonite, 10 mm
Äspö	KA2423A04	2,77	50	1	1 mm clay min
Äspö	KA2423A04	3,02	90	1	

A2c Fracture mapping, continued

Site	Hole ID	Depth	Angle vs hole axis	Quantity	Remark
Äspö	KA2549A01	0,05	40	1	no visible minerals, slight surface stain
Äspö	KA2549A01	0,10	35	1	no visible minerals, slight surface stain
Äspö	KA2549A01	0,10	35	1	no visible minerals, slight surface stain
Äspö	KA2549A01	0,14	30	1	no visible minerals, slight surface stain
Äspö	KA2549A01	0,25	65	1	no visible minerals, slight surface stain
Äspö	KA2549A01	0,30	90	1	no visible minerals, slight surface stain
Äspö	KA2549A01	0,35	90	1	no visible minerals, slight surface stain
Äspö	KA2549A01	0,62	40	1	no visible minerals, slight surface stain
Äspö	KA2549A01	0,65	60	1	no visible minerals, slight surface stain
Äspö	KA2549A01	0,81	50	1	no visible minerals, slight surface stain
Äspö	KA2549A01	1,10	73	1	no visible minerals, slight surface stain
Äspö	KA2549A01	1,30	70	1	no visible minerals, slight surface stain
Äspö	KA2549A01	3,10	40	1	no visible minerals, slight surface stain
Äspö	KA2549A01	3,25	40	1	no visible minerals, slight surface stain
Äspö	KA2549A02	0,05	80,00	1	no visible minerals, slight surface stain
Äspö	KA2549A02	0,25	85	1	no visible minerals, slight surface stain
Äspö	KA2549A02	0,32	70	1	no visible minerals, slight surface stain
Äspö	KA2549A02	0,48	50	1	no visible minerals, slight surface stain
Äspö	KA2549A02	0,53	60	1	no visible minerals, slight surface stain
Äspö	KA2549A02	0,72	70	1	no visible minerals, slight surface stain
Äspö	KA2549A02	0,87	80	1	no visible minerals, slight surface stain
Äspö	KA2549A02	1,00	70	1	no visible minerals, slight surface stain
Äspö	KA2549A02	1,05	50	1	no visible minerals, slight surface stain
Äspö	KA2549A02	1,10	90	1	no visible minerals, slight surface stain
Äspö	KA2549A02	1,28	90	1	no visible minerals, slight surface stain
Äspö	KA2549A02	1,33	30	1	no visible minerals, slight surface stain
Äspö	KA2549A02	1,44	90	1	no visible minerals, slight surface stain
Äspö	KA2549A02	1,57	30	1	no visible minerals, slight surface stain
Äspö	KA2549A02	1,93	90	1	no visible minerals, slight surface stain
Äspö	KA2549A02	1,97	50	1	no visible minerals, slight surface stain
Äspö	KA2549A02	2,25	35	1	no visible minerals, slight surface stain
Äspö	KA2549A02	3,10	70	1	no visible minerals, slight surface stain
Äspö	KA2549A02	3,25	38	1	no visible minerals, slight surface stain
Äspö	KA2549A02	3,45	40	1	no visible minerals, slight surface stain
Äspö	KA2549A02	3,50	80	1	no visible minerals, slight surface stain
Äspö	KA2549A02	3,55	10	1	no visible minerals, slight surface stain
Äspö	KA2549A02	3,65	50	1	no visible minerals, slight surface stain
Äspö	KA2549A02	3,85	70	1	no visible minerals, slight surface stain
Äspö	KA2549A02	3,95	70	1	no visible minerals, slight surface stain
Äspö	KA2549A02	4,68	60	1	no visible minerals, slight surface stain
Äspö	KA2549A02	4,83	25	1	no visible minerals, slight surface stain
Äspö	KA2549A03	0,17	80	1	no visible minerals, slight surface stain
Äspö	KA2549A03	0,22	65	1	no visible minerals, slight surface stain
Äspö	KA2549A03	0,91	30	1	no visible minerals, slight surface stain
Äspö	KA2549A03	1,00	35	1	no visible minerals, slight surface stain
Äspö	KA2549A03	1,55	50	1	no visible minerals, slight surface stain
Äspö	KA2549A03	2,05	45	1	no visible minerals, slight surface stain
Äspö	KA2549A03	2,50	75	1	no visible minerals, slight surface stain
Äspö	KA2549A03	3,35	30	1	no visible minerals, slight surface stain
Äspö	KA2549A03	4,31	50	1	no visible minerals, slight surface stain
Äspö	KA2549A03	4,42	40	1	no visible minerals, slight surface stain
Äspö	KA2548A01	0,12	50	1	no visible minerals, slight surface stain
Äspö	KA2548A01	0,15	70	1	no visible minerals, slight surface stain
Äspö	KA2548A01	0,20	30	1	no visible minerals, slight surface stain
Äspö	KA2548A01	0,25	70	1	no visible minerals, slight surface stain
Äspö	KA2548A01	1,10	70	1	no visible minerals, slight surface stain
Äspö	KA2548A01	1,45	40	1	no visible minerals, slight surface stain
Äspö	KA2548A01	1,58	45	1	chlorite, thin coating
Äspö	KA2548A01	1,98	38	1	no visible minerals, slight surface stain
Äspö	KA2548A01	2,44	35	1	chlorite, thin coating and calcite
Äspö	KA2548A01	3,00	45	1	no visible minerals, slight surface stain
Äspö	KA2548A01	4,10	70	1	no visible minerals, slight surface stain
Äspö	KA2548A01	4,55		1	no visible minerals, slight surface stain

A2d: RQD

Site	Hole ID	secup	seclow	total cm	<10 cm	> 10cm	RQD %
Äspö	KA1596A01	0,00	5,70	570		570	90
Äspö	KA1596A02	0,00	5,62	562	140	422	91
Äspö	KA1596A03	0,00	4,80	480	100	380	79
Äspö	KA1596A04	0,00	4,04	404		177	44
Äspö	KA2169A01	0,00	3,62	362	50	312	86
Äspö	KA2169A02	0,00	4,32	432	80	352	81
Äspö	KA2169A03	0,00	4,28	428	20	408	95
Äspö	KA2169A04	0,00	5,47	547	5	542	99
Äspö	KA2423A01	0,00	5,04	504	20	484	96
Äspö	KA2423A02	0,00	3,67	367	55	312	85
Äspö	KA2423A03	0,00	2,93	293	25	268	91
Äspö	KA2423A04	0,00	3,11	311	15	296	95
Äspö	KA2548A01	0,00	4,65	465	25	440	95
Äspö	KA2549A01	0,00	3,69	369	70	299	81
Äspö	KA2549A02	0,00	5,21	521	90	431	83
Äspö	KA2549A03	0,00	5,50	550	10	540	98
Total hole length				71,65			

A2e: Details on fault zones

Site	Hole ID	secup	seclow	Zone type	Matrix %	Clast size, mm	angle to axis
Äspö	KA1596A01	4,52	4,54	fault crush	<10	2 to 10	90
Äspö	KA1596A01	5,25	5,30	fault gouge & mylonite	ca 100		35
Äspö	KA1596A01	5,48	5,62	fault breccia	ca 50	ca 10	40
Äspö	KA1596A02	4,50	4,84	fault gouge			40
Äspö	KA1596A02	5,12	5,62	chlorite phyllite			60
Äspö	KA1596A03	3,14	3,18	fault gouge			30
Äspö	KA1596A03	3,36	3,52	fault gouge			30
Äspö	KA1596A03	4,15	4,22	fault gouge			30
Äspö	KA1596A04	2,32	2,36	fault gouge			30
Äspö	KA1596A04	2,44	2,52	fault gouge			30
Äspö	KA1596A04	2,72	2,80	fault gouge			30
Äspö	KA2169A01	1,62	1,66	cataclasite	70	<5x10 mm	33
Äspö	KA2169A01	2,47	2,49	Fault crush of cataclasite	70		40
Äspö	KA2169A02	1,90	1,91	cataclasite 10 mm green			50
Äspö	KA2169A02	2,96	3,10	Fault crush	0	20 mm	30
Äspö	KA2169A02	3,88	3,88	cataclasite 2-4 mm			60
Äspö	KA2169A02	3,94	3,94	cataclasite 2-4 mm			40
Äspö	KA2169A02	3,96	4,00	fractured cataclasite	70		32
Äspö	KA2169A03	3,95	3,98	fault breccia in cataclasite		flaky <5x20 mm	30
Äspö	KA2169A04	2,87	2,88	Fault crush		flaky <5x20 mm	40
Äspö	KA2169A04	2,89	2,89	cataclasite 2-3 mm			60
Äspö	KA2169A04	2,97	2,97	cataclasite 5 mm			50
Äspö	KA2169A04	3,58	3,58	cataclasite 1 mm			60
Äspö	KA2169A04	3,76	3,77	cataclasite 1 mm			60
Äspö	KA2169A04	3,80	3,80	cataclasite 1 mm			60
Äspö	KA2169A04	3,87	3,87	cataclasite 1 mm			60
Äspö	KA2169A04	4,47	4,47	cataclasite 1 mm			60
Äspö	KA2423A01	3,96	4,00	Mylonite	ca 70	2 to 5	51
Äspö	KA2423A01	4,00	4,05	Protocataclasite			40
Äspö	KA2423A01	4,05	4,07	Mylonite	ca 70	2 to 5	25
Äspö	KA2423A01	4,07	4,22	cataclasite	10 to 20		40
Äspö	KA2423A01	4,22	4,26	Mylonite & fault gouge	ca 70	2 to 5	35
Äspö	KA2423A01	4,26	4,33	cataclasite	10 to 20		40
Äspö	KA2423A02	2,72	2,75	fault gouge	> 50	ca 5	38
Äspö	KA2423A03	2,36	2,37	fault crush	<10		40
Äspö	KA2423A03	2,40	2,41	fault crush	<10		40
Äspö	KA2423A03	2,52	2,53	fault crush			50
Äspö	KA2423A04	1,92	1,94	fault crush	ca 10	ca 5	60
Äspö	KA2549A01	1,86	1,87	ultracataclasite 4 to 12 mm	5	< 1	7
Äspö	KA2549A01	1,87	1,88	cataclasite < 6 mm	20	1 to 2	7
Äspö	KA2549A01	1,98	1,99	fault crush 5 mm	< 5	1 to 4	25
Äspö	KA2549A01	2,02	2,03	fault crush 5 mm, parallel with the former	< 5	1 to 4	25
Äspö	KA2549A01	2,12	2,15	fault crush 5 mm, subparallel with the former	< 5	1 to 4	10
Äspö	KA2549A02	2,35	2,35	mylonite, 2 mm	ca 100	zero	10
Äspö	KA2549A02	3,55	3,57	cataclasite			10
Äspö	KA2549A02	4,45	4,46	mylonite, 2-7 mm			
Äspö	KA2549A03	1,85	1,86	mylonite, 2-5 mm			30
Äspö	KA2548A01	1,58	1,62	Fault crush of cataclasite	0	< 5x40 mm	33

A2f: Water inflow

Site	**Hole ID**	Date	Time	Flow (l/min)	Remark
Äspö	KA1596A01	03-03-30	15:35	600	at 5,5 m
Äspö	KA1596A02	03-03-30	17:00	0	no flow observed during drilling
Äspö	KA1596A03	03-03-30	15:30	4	no flow observed during drilling
Äspö	KA1596A04	03-03-30	17:00	0	no flow observed during drilling
Äspö	KA2169A01	03-04-06	08:20	235	no flow observed during drilling
Äspö	KA2169A02	03-04-06	08:10	235	no flow observed during drilling
Äspö	KA2169A03	03-04-06	08:00	250	no flow observed during drilling
Äspö	KA2169A04	03-04-07	09:30	0	no flow observed during drilling
Äspö	KA2423A01	03-03-22	12:00	23	no flow observed during drilling
Äspö	KA2423A02	03-03-22	15:05	0	no flow observed during drilling
Äspö	KA2423A03	03-03-22	15:00	13	no flow observed during drilling
Äspö	KA2423A04	03-03-23	13:45	0	no flow observed during drilling
Äspö	KA2548A01	03-04-07	11:00	0	no flow observed during drilling
Äspö	KA2549A01	03-04-07	11:00	0	no flow observed during drilling
Äspö	KA2549A02	03-04-07	11:00	950	after last round: 3,88-5,21
Äspö	KA2549A03	03-04-07	11:00	0	no flow observed during drilling

Appendix 3 Structural geological map of drill cores KA1596, KA2169, KA2423 and KA2549

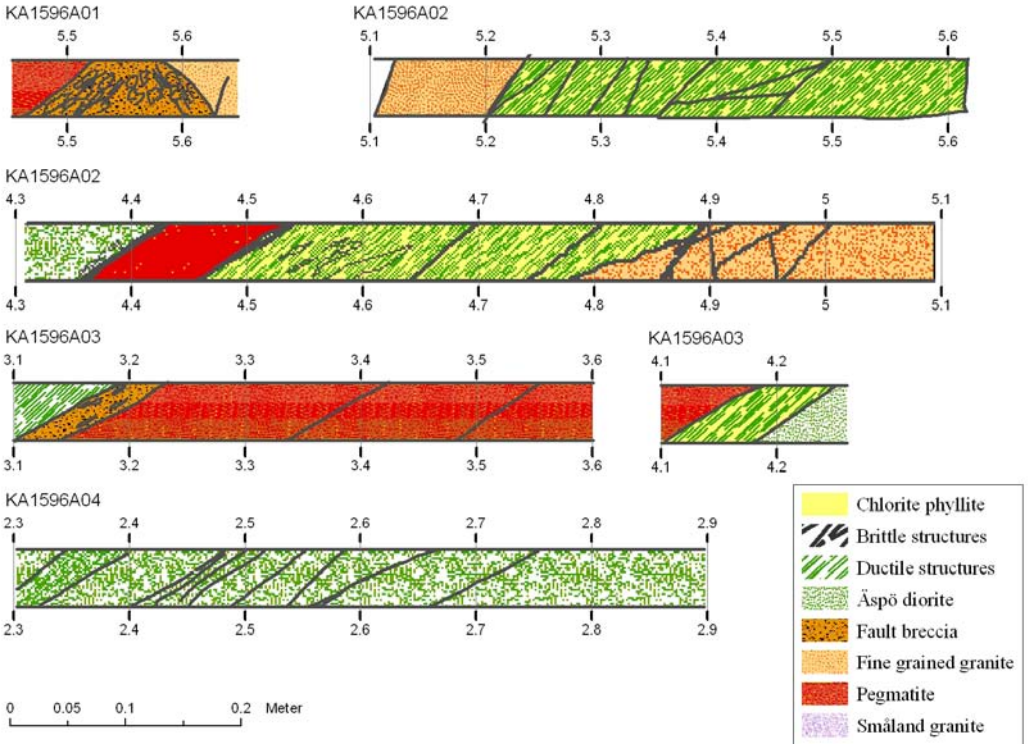

Figure A3-1. *Structural geological map of drill cores KA1596A01 through KA1596A04.*

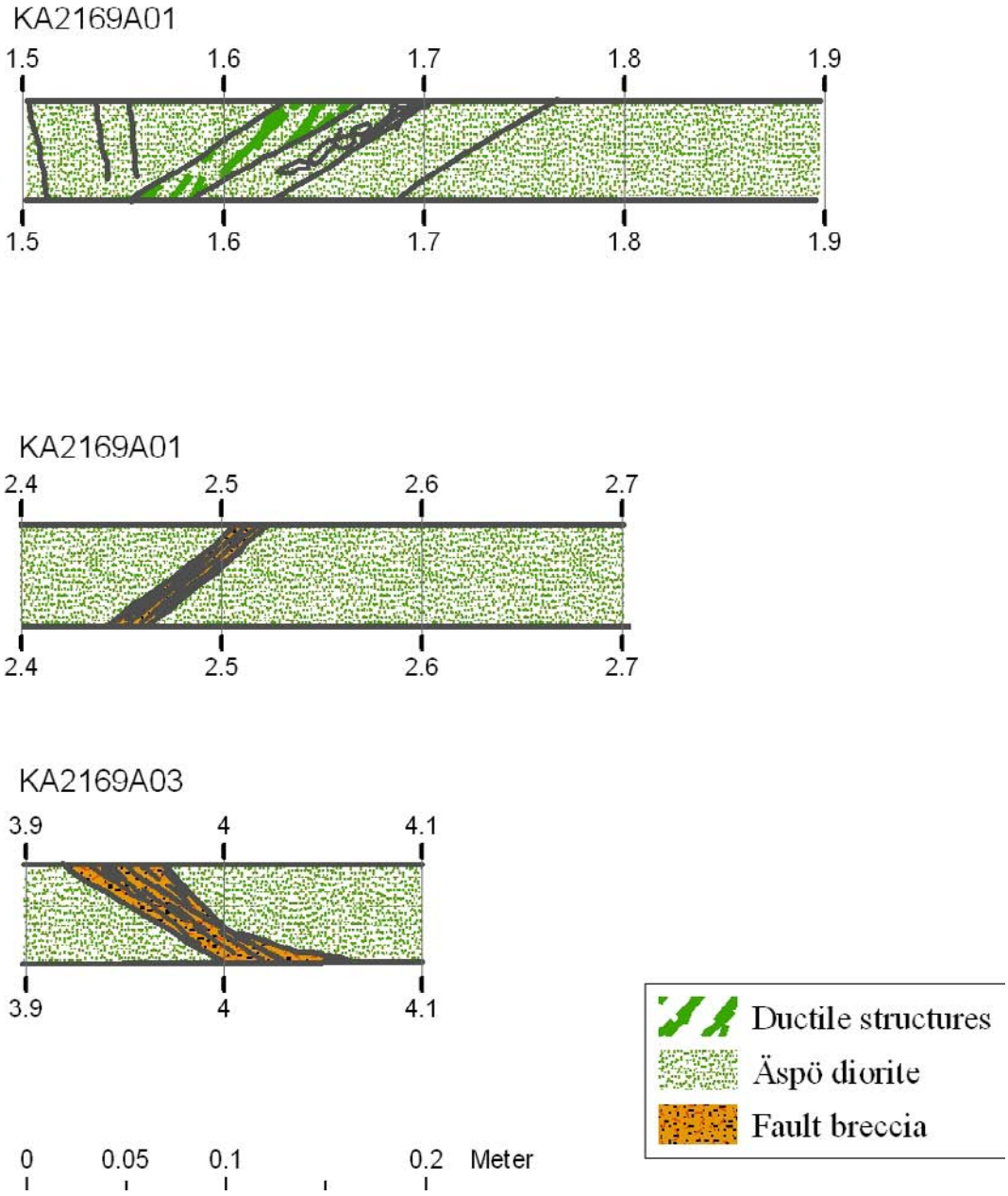

Figure A3-2. *Structural geological map of drill cores KA2169A01 and KA2169A03.*

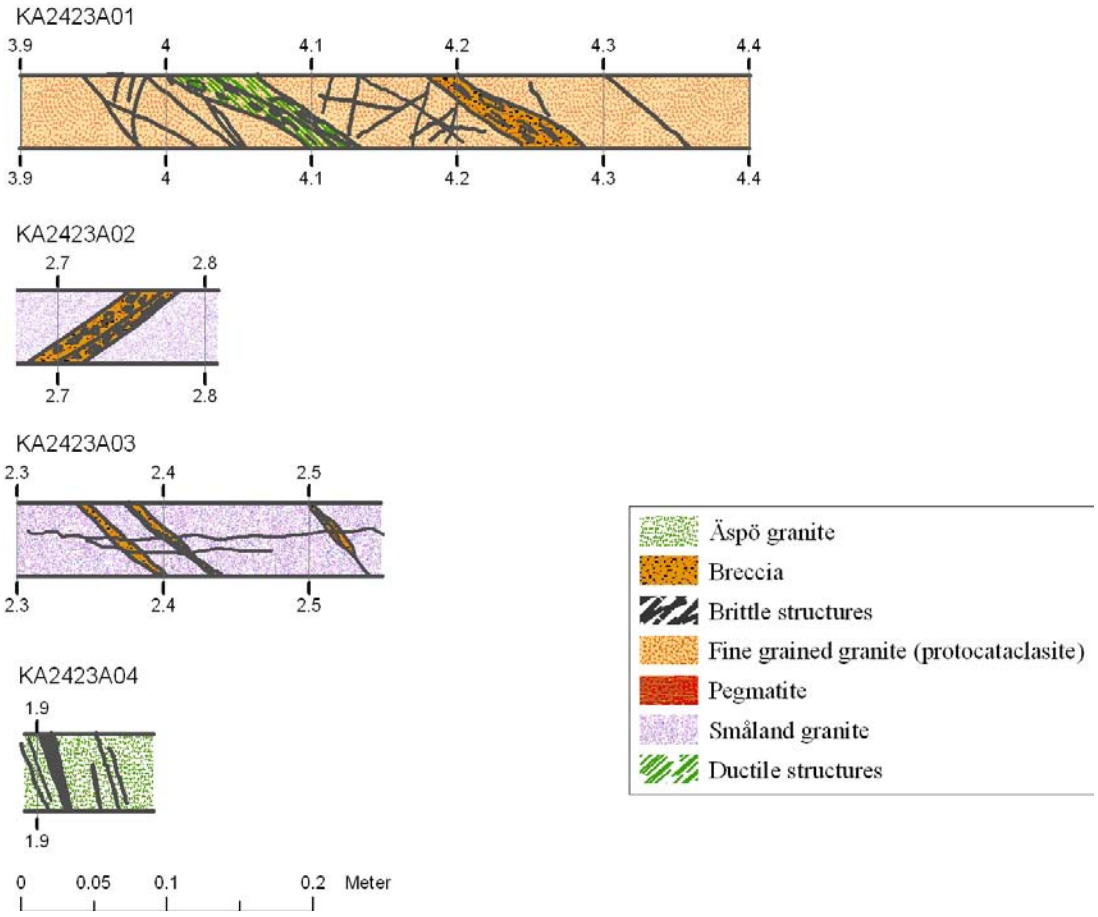

Figure A3-3. *Structural geological map of drill cores KA2423A01 through KA2423A04.*

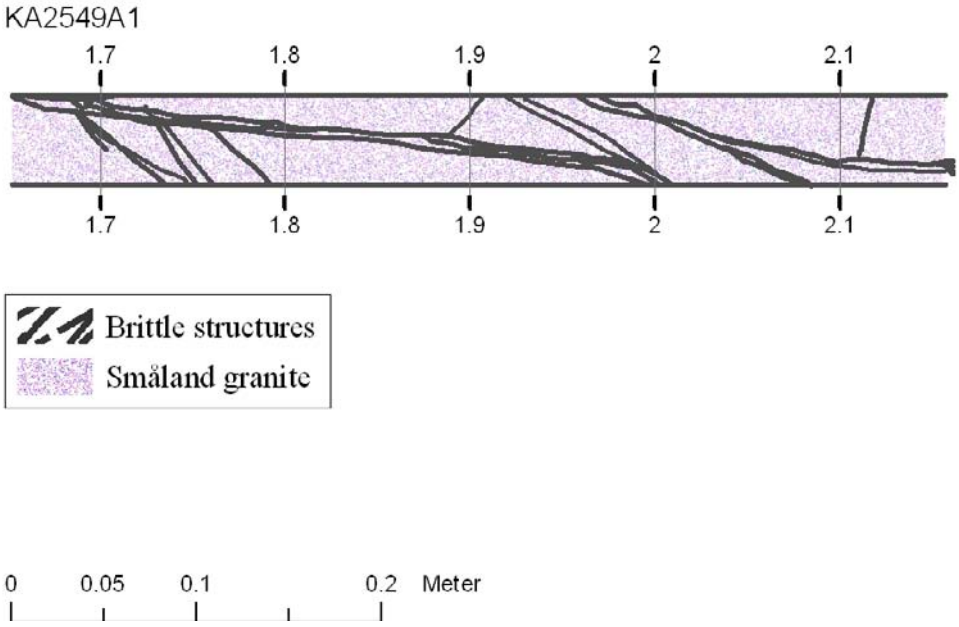

Figure A3-4. *Structural geological map of drill core KA2549A01.*

Appendix 4 Detailed geological map of the tunnel wall of each candidate zone

The four zones at chainages 1/600 m, 2/163 m, 2/430 m, and 2/545 m were mapped in detail on Wall A. The results are shown on the maps. Orientations of fractures and faults were measured and are shown below in Table A4-1. Capital letters refer to individual structures in the maps.

Table A4-1. Key to zone notation in detailed maps of zone exposures

Site	ID	Strike	Dip
2430	A	194	66
2430	B	300	30
2430	C	200	40
2430	D	210	30
2430	E	170	80
2430	F	174	85
2430	G	184	70
2430	H	120	20
1600	not labeled	0	0
1600	not labeled	100	85
2545	A	314	56
2545	B	185	15
2545	C	304	85
2545	D	185	10
2545	E	310	80
2545	F	275	50
2545	G	280	72
2545	H	250	30
2545	I	326	75
2163	A	150	80
2163	B	130	80
2163	C	130	80
2163	D	40	70
2163	E	40	70
2163	F	40	70
2163	G	124	82
2163	H	130	80
2163	I	8	80
2163	not labeled	140	50
2163	not labeled	40	70

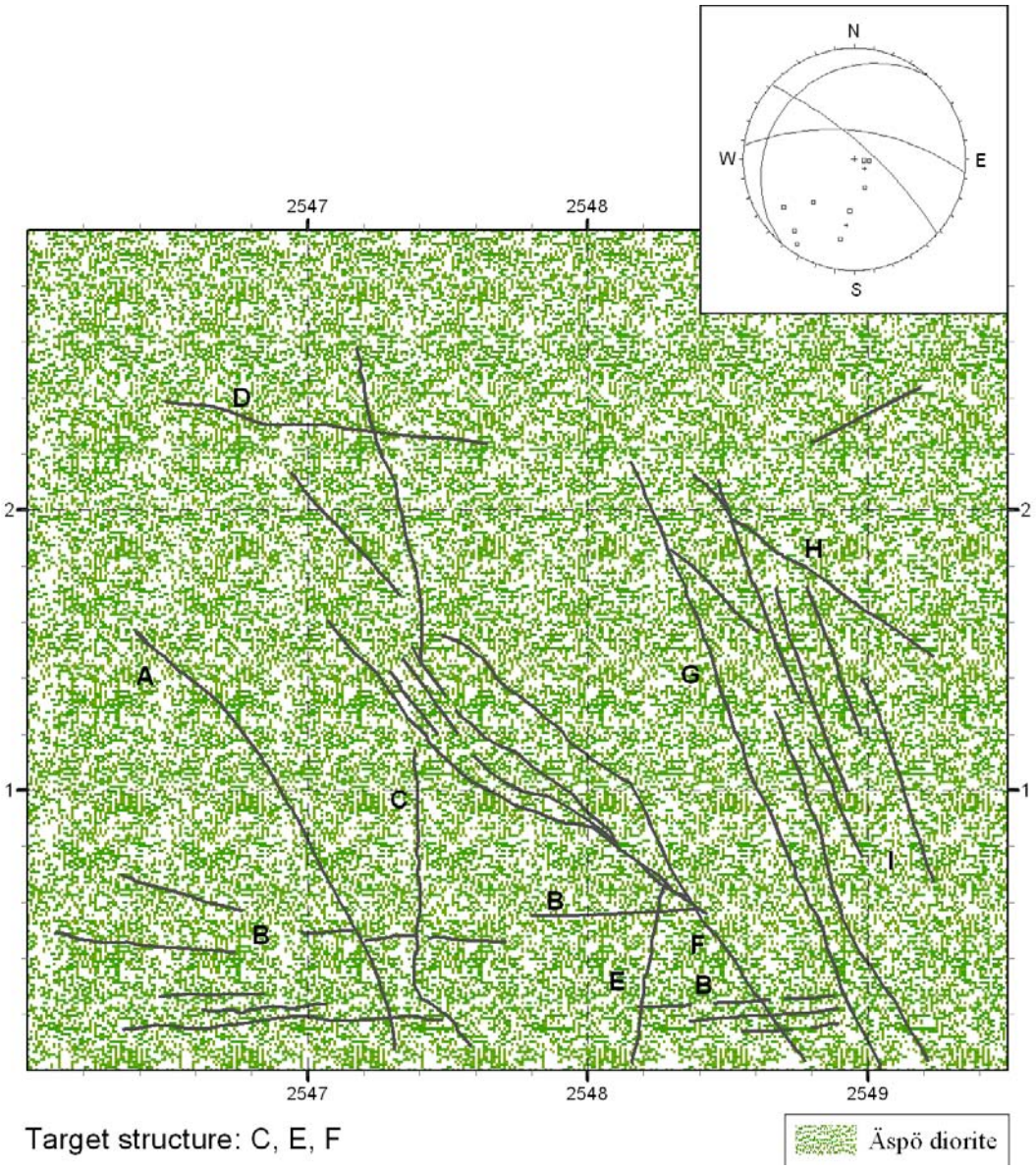

Figure A4- 1. *Structural geological map of tunnel section 2/545 m.*

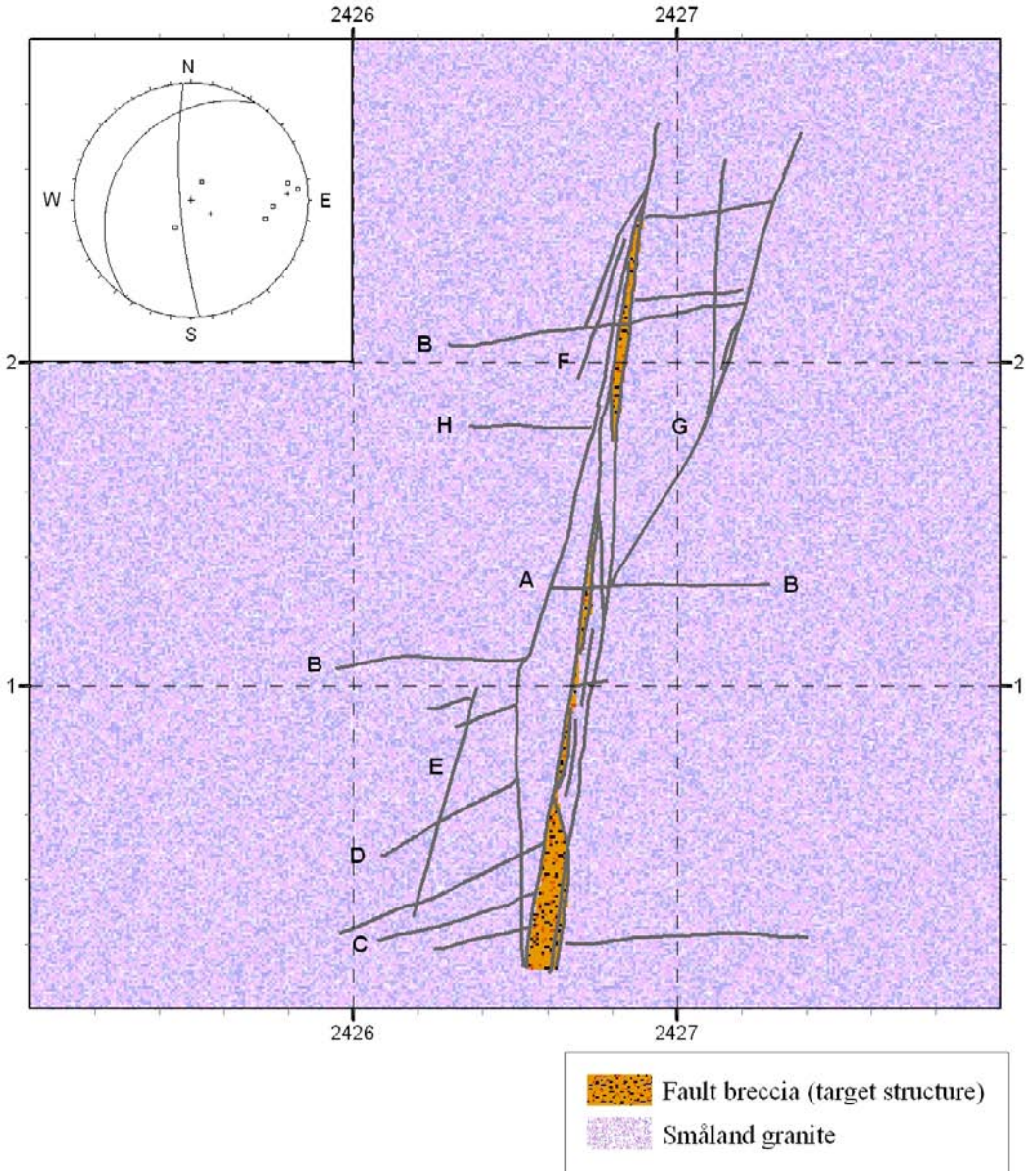

Figure A4-2. *Structural geological map of tunnel section 2/430 m.*

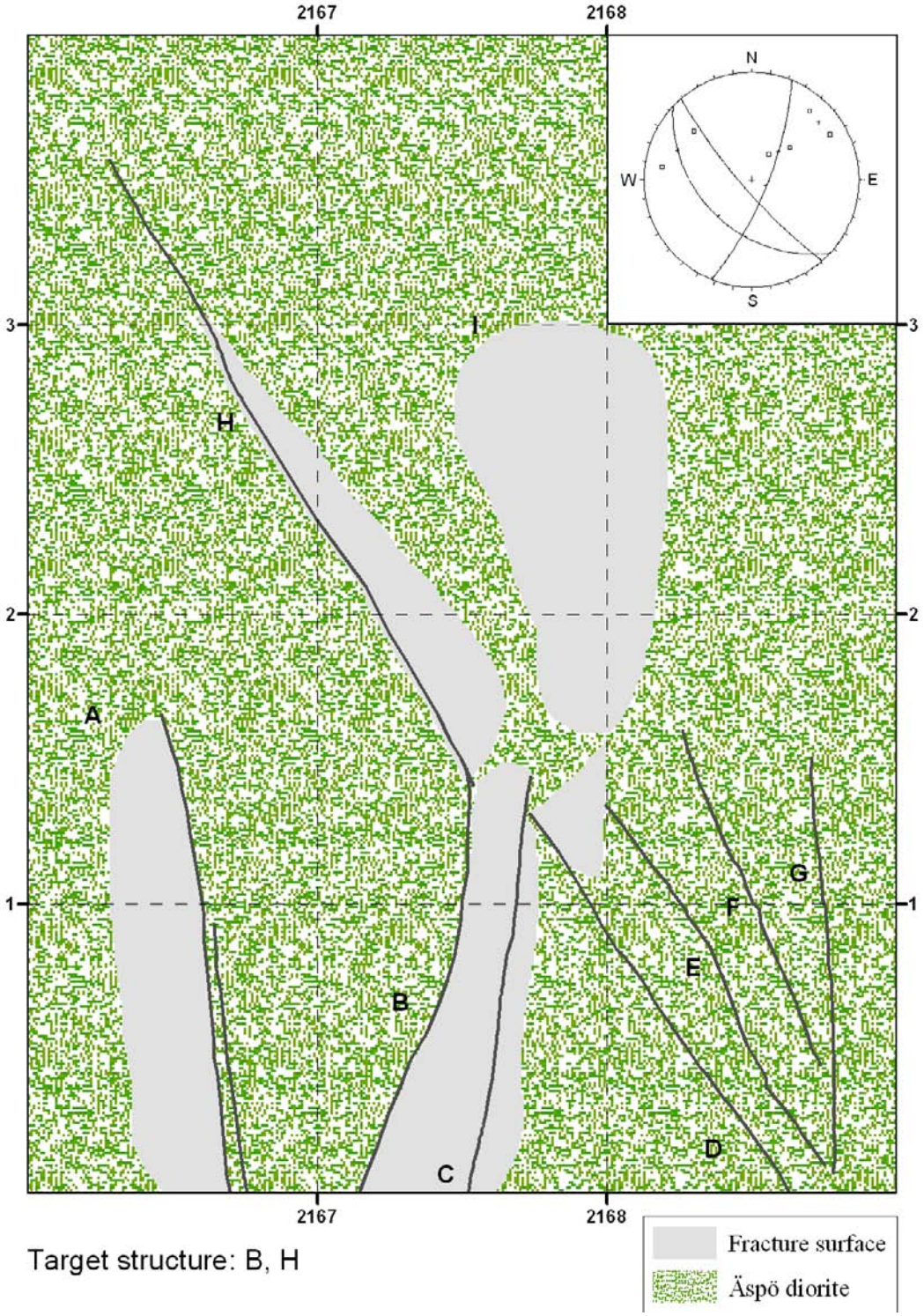

Figure A4-3. *Structural geological map of tunnel section 2/163 m.*

Appendix 4. Detail map of zone exposures in Tunnel

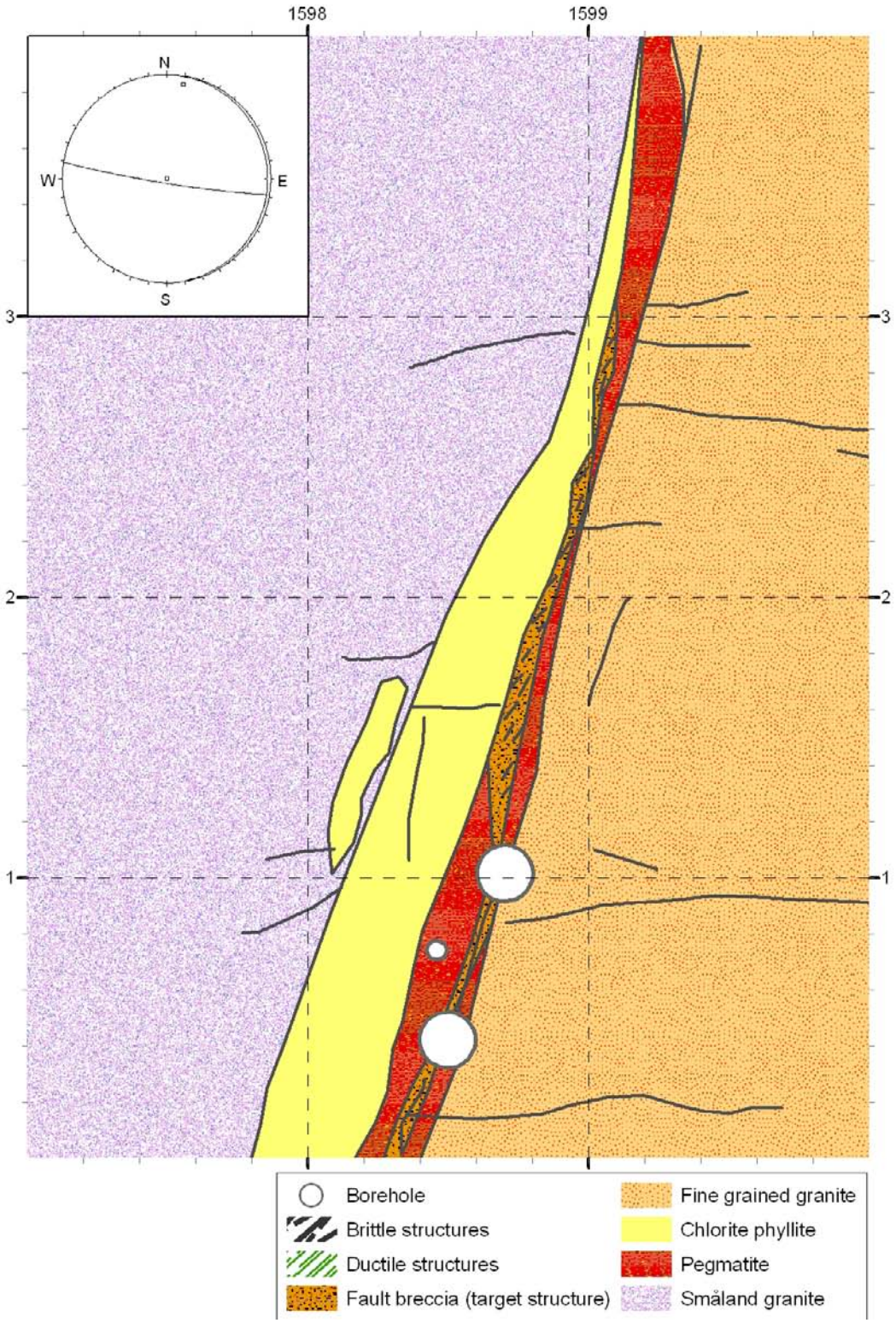

Figure A4-4. *Structural geological map of tunnel section 1/600 m.*

Appendix 5: IPC analysis of samples from KA1596A01, KA2169A02 and KA2423A03

Element analyses

ELEMENT	SAMPLE	KA1596A01	KA2169A02	KA2423A03
TS	%	95,9	98,4	98,4
SiO2	% TS	38,1	41,8	21,2
Al2O3	% TS	15,4	14,7	5,73
CaO	% TS	3,33	10,3	39,8
Fe2O3	% TS	12,8	10,2	3,43
K2O	% TS	3,65	1,83	2,93
MgO	% TS	14,6	7,12	2,76
MnO	% TS	0,306	0,178	0,111
Na2O	% TS	0,252	2,84	0,343
P2O5	% TS	0,224	0,446	0,0513
TiO2	% TS	0,854	1,25	0,145
Summa	% TS	89,5	90,7	76,5
Ba	mg/kg TS	460	612	450
Be	mg/kg TS	7,88	2	1,58
Co	mg/kg TS	46,5	18,8	7,17
Cr	mg/kg TS	960	233	13,7
Cs	mg/kg TS	2,14	<0,1	<0,1
Cu	mg/kg TS	47	148	67
Ga	mg/kg TS	47,6	61,6	<1
Hf	mg/kg TS	3,86	7,8	19,1
Mo	mg/kg TS	<2	<2	<2
Nb	mg/kg TS	9,49	12,9	7,33
Ni	mg/kg TS	416	129	<10
Rb	mg/kg TS	154	59	51,2
S	mg/kg TS	323	1280	3580
Sc	mg/kg TS	20,1	14,9	3,45
Sn	mg/kg TS	11,1	8,87	1,56
Sr	mg/kg TS	296	1440	362
Ta	mg/kg TS	1,23	0,665	4,98
Th	mg/kg TS	9,78	3,2	6,58
U	mg/kg TS	4,25	3,14	0,551
V	mg/kg TS	158	159	84,1
W	mg/kg TS	6,5	150	179
Y	mg/kg TS	15,5	26,4	78,3
Zn	mg/kg TS	443	438	122
Zr	mg/kg TS	124	340	49,1

Analyses performed by Analytica AB
Ordernumber: L0306303
Report created: 2003-07-30

Analyses of lantanides

ELEMENT	SAMPLE	KA1596A01	KA2169A02	KA2423A03
La	mg/kg TS	26,3	67,8	25,9
Ce	mg/kg TS	53,6	140	52,5
Pr	mg/kg TS	<1	7,96	<1
Nd	mg/kg TS	20,8	65,9	18,5
Sm	mg/kg TS	2,83	7,14	0,932
Eu	mg/kg TS	0,381	1,02	<0,05
Gd	mg/kg TS	<0,4	2,55	<0,4
Tb	mg/kg TS	<0,1	<0,1	<0,1
Dy	mg/kg TS	1,97	3,09	4,49
Ho	mg/kg TS	0,404	0,518	0,855
Er	mg/kg TS	<0,1	<0,1	<0,1
Tm	mg/kg TS	<0,1	<0,1	<0,1
Yb	mg/kg TS	<0,2	0,637	1,43
Lu	mg/kg TS	0,101	0,0555	0,184

Analyses performed by Analytica AB
Ordernumber: L0306345
Report created: 2003-07-30

Appendix 6: XRD analysis on samples from KA1596A01, KA2169A02 and KA2423A03

XRD-analysis of ≥2 μm and <2 μm fractions from three fracture filling samples from the investigated fault rock zones at Äspö HRL.

Three samples from KA1596A01 (0.91 g), KA2169A02 (0.90 g) and KA2423A03 (0.47 g) were prepared and used for XRD-analysis performed by Sven Snäll of the Geological Survey of Sweden, Uppsala.

Fractionation

Sedimentation of suspended particles was carried out in a beaker with distilled water using ultrasonic treatment. Separation was carried out of particles <2 μm from those ≥2 μm resulting in the following fractions:

Sample	<2 μm (weight-%)	≥2 μm (weight-%)
KA1596A01	70.5	29.5
KA2169A02	78.8	21.2
KA2423A03	82.0	18.0

Analyses

The analyses were carried out using a Siemens D 5000 (theta-theta) diffractometer with CuKα and graphite monochromator. A voltage of 40 kV and a current of 40 mA were used. Spectra within the 2-theta interval 2-65 deg were used for randomly orientated particles of the ≥2 μm fractions. Concerning clay particles (orientated particles) the 2-thweta interval 2-35 deg was used. The sweep rate was 0.02 degrees/2 sec. The analyses of particles ≥2 μm were carried out with rotating sample holders and variable divergence aperture. The clay minerals were analysed using fixed sample holder and 1 deg. divergence aperture. In both cases a 2 mm receiving aperture was mounted in the beam.

Evaluation

The Bruker/Siemens DIFFRACplus software (version 2.2; programme EVA) was used for the evaluation. The work of /Brindley and Brown, 1984/ and /Jasmund and Lagaly, 1993/ were used for mineral identification of clay minerals.

Results

Evaluated raw files were delivered of which here follows a short summary:

Sample KA1596A01

Fraction <2 μm

A swelling mineral, similar to corrensite was detected with 001-peak at 30.4 Å, 002-peak at 15.1 Å and 004 peak at 7.58 Å at EG-saturation. The d-values deviate somewhat from corrensite of /Jasmund and Lagaly, 1993/ p. 461. Enhanced intensity within the 14 Å-12 Å interval of the heated sample (400 ^{o}C) indicates a clay mineral consisting of alternating layers with chlorite and smectite structures, alternatively chlorite and vermiculite structures, like in corrensite, although the components are not so ordered as in pure corrensite. Possibly the proportions between swelling and none-swelling layers are different from that in corrensite. The analyses also show that the samples contain considerable amounts of pure chlorite, with peaks at 14.1 Å – 14.2 Å and 7, 11 Å.

Fraktion ≥2 μm

The coarse material consists of quartz, K-feldspar, calcite, much of chlorite and somewhat of illite. Small amounts of the mixed-layer minerals may also be present in this coarse fraction but has not been specifically (EG-saturation) analysed.

Sample KA2169A02

Fraction <2 μm

This material also contains a corrensite-like swelling mineral with a 001-peak at 30.4 Å, a 002-peak at 15.4 Å and a 004 peak at 7.72 Å at EG-saturation. The d-values deviate somewhat from those of /Jasmund and Lagaly, 1993, p. 461 (corrensite)/. Enhanced intensity at 14 Å through 12 Å in the XRD-spectrum for the heated sample (400 ^{o}C) reveals a mixed-layer mineral similar to that found in the KA1596A01 sample. Possibly, the proportions between swelling and none-swelling layers are different from that in corrensite. The analyses also show that the samples contain considerable amounts of pure chlorite, with peaks at 14.1 Å – 14.2 Å and 7. 11 Å

Fraction ≥2 μm

This material consists of quartz, plagioclase, calcite, some K-feldspar and illite and probably also epidote and large amounts of chlorite. Small amounts of the mixed-layer mineral may also be present in this coarse fraction but has not been specifically (EG-saturation) analysed concerning identification of clay minerals.

The illite may be of the muscovite type but is not possible to identify from the XRD-diagram since the typical muscovite 002-peak at 5 Å (17.8^{o} 2θ) overlaps a epidote peak.

Sample KA2403A03

Fraction <2 μm

The major mineral is chlorite but also a swelling mineral with a peak at 14.4 Å is present in the untreated sample, and at 16.2 Å at EG saturation. A high background in the heated sample within the 6-9.5 Å ($^{o}2\theta$ interval) suggests different components of for example chlorite, smectite or vermiculite but possibly also illite. The lack of a distinct peak indicates a disordered arrangement of the mixed layer mineral(s).

The 3.15 Å peak is related to fluorite.

Fraction ≥2 μm

This coarser material mainly consists of fluorite and calcite. Small amounts of quartz and K-feldspar are present.

References

Brindley, G.W. and G. Brown 1984. Crystal structures of clay minerals and their X-ray identification. – Mineralogical Society, Monograph no. 5, Mineralogical Society, 41 Queen's Gate, London SW7 5HR.

Drever, S.I. 1973. The preparation of oriented clay mineral specimens for X-ray diffraction analysis by a filter-membrane peel technique. – Am. Miner., 58, 553-554.

Jasmund, K. and G. Lagely 1993. Tonminerale und Tone. – Steinkopff Verlag Darmstadt. (in German).